Volume 17, Issue 4, 172531 (1-21)

Iranian Journal of Earth Science (IJES)

https://doi.org/10.57647/j.ijes.2025.16900

Eocene volcanism in the Tashvir region: Indication of extension in the Northern subzone of the Tarom range in northwestern Iran

Reza Jamalomidi[1], Saeid Hakimi Asiabar[1,*], Sharoz Haghnazar[1], Mansor Vosoghi Abedini[2]

[1]*Department of Geology, La.C., Islamic Azad University, Lahijan, Iran.*
[2]*Department of Geology, SR.C., Islamic Azad University, Tehran, Iran.*

[*]**Corresponding author:** saeid.h.asiabar@gmail.com

Original Research

Received:
2024-03-09
Revised:
2024-05-13
Accepted:
2024-07-28
Published online:
2025-06-08
Published in issue:
2025-10-30

Abstract:

The present study aims to characterize the igneous rocks of the Tashvir range. The Tarom mountains are located at the southwest end of the Alborz mountain range with an approximate northwest-southeast orientation. Tashvir region is part of the northern edge of the Tarom mountains and 90 km northeast of Zanjan city. Igneous rocks of this range mainly include basalt, basaltic andesite, and interlayers of tuff. Petrographically, these rocks contain olivine and clinopyroxene phenocrysts with a zoning structure. Since they have olivine and nepheline (less than 5%) in their norms, they can be considered alkali olivine basalts. A remarkable feature of olivines in the Tarom basalts is the presence of carbonate fragments that have reacted with magma and completely turned into clinopyroxene needles. The reduction in SiO_2 concentration and the reduction in Mg# concentration suggest the assimilation of carbonate rocks by basaltic magma. Also, the pattern of enrichment in large-ion lithophile elements (LILEs), the positive anomalies of Ce, P, and Sm, the depletion of Nb, Ta, Zr, Hf, and Th elements, and Low K_2O/Na_2O and Ba/Rb ratios in the rock samples of the Tashvir range indicate magma contamination with the lower crust. The evidence of crustal contamination and Nb/Y and Zr/Y values in the samples indicate that the primary origin of the basalts in the Tashevir region is due to plume sources. The alkaline nature, shoshonitic, peraluminous nature, and low Ti content of the rocks of the Tashvir area, along with enrichment in the rare earth elements (REE) and other elements such as Ba, Rb, Sr as well as the magma origin and depth of magma generation suggest that these magmas belong to an original rift environment. The tectonic setting of the Tarom range is divided into two parallel sub-ranges with arc-type eruptions and rift zones, where the expansion of this rift zone has stopped before developing into a back-arc basin.

Keywords: Petrology; Basalt; Rift; Tarom Mountains; Alborz

1. Introduction

Iran's magmatism in the Cenozoic has been of special importance due to its appearance in both volcanic and plutonic forms and making the largest outcrops of Iran's igneous rocks (Fig. 1). These magmatic activities have been observed in most structural zones of Iran, except Zagros and Kopet Dagh, with the peak volcanism having occurred in the Eocene and the highest plutonism intensity in the Oligocene and Miocene (Emami, 2000; Ghorbani, 2013; Abdolahadi et al., 2025; Salehpour et al., 2025; Elmi et al., 2025). Tertiary mafic volcanic rocks in northern Alborz Iran are believed to be the result of the subduction of Neo-Tethys (Alavi, 1996). The Alborz Mountains accommodate the motion between the South Caspian Basin (SCB) and Central Iran. The Alborz Mountains, which belong to the Alpine-Himalayan belt, were folded during Late Alpine orogeny and are tectonically active (Ritz et al., 2006). The Alpine orogeny began, therefore, with Eocene volcanism in southwestern and south-central parts of the Alborz, and continued with the uplift and folding of the older sedimentary rocks in the northwestern, central, and eastern parts of the range, during

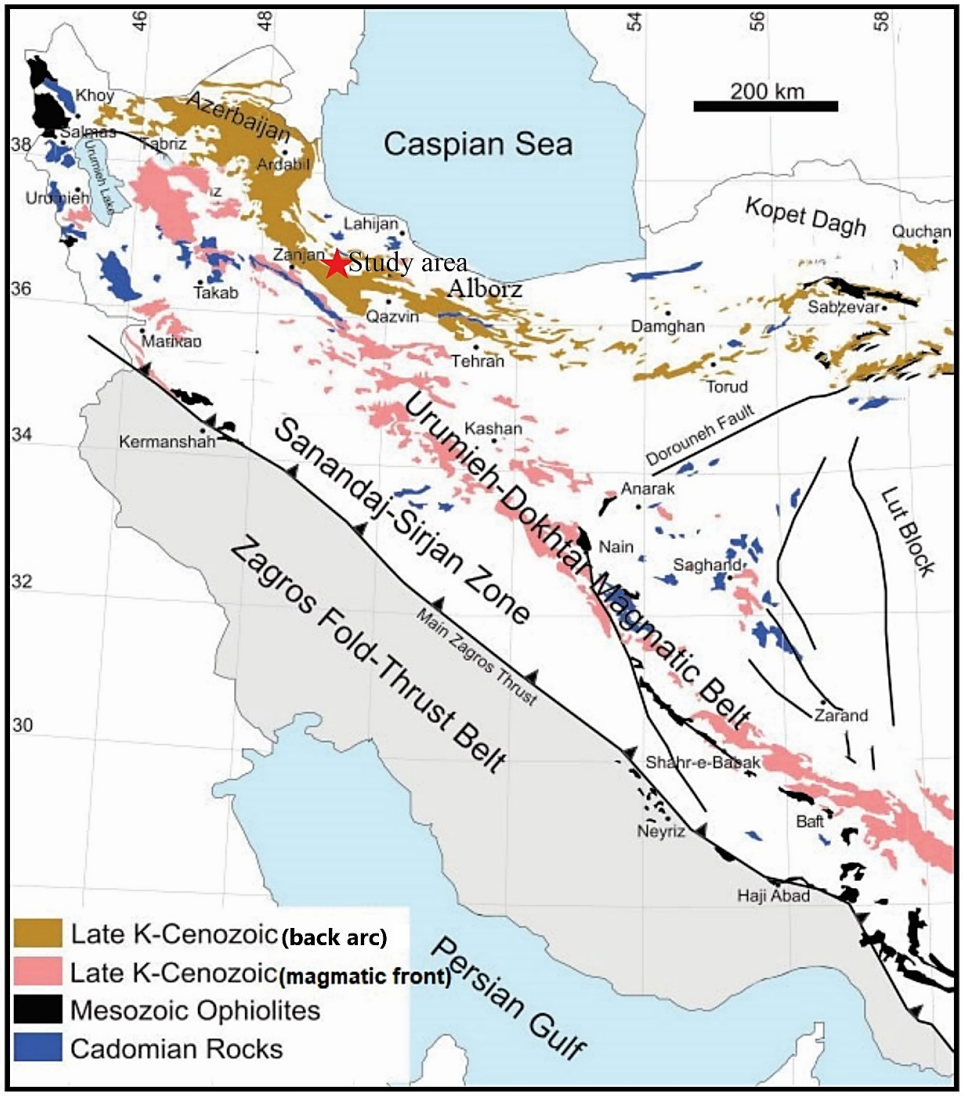

Figure 1. Simplified geological map of Iran emphasizing Ediacaran-Early Cambrian (Cadomian) magmatic rocks, Mesozoic ophiolites, and Cenozoic magmatic rocks from back-arc and magmatic front (after Shafaii Moghadam et al. (2020)).

the most important orogenic phases, which date from the Miocene and Pliocene epochs.

In the Eocene, due to the subduction of Neo-Tethys, a back-arc basin was formed. The crust tensional stress results in the subsidence generating the current southern Alborz (Berberian and King, 1981).

The region's tensile behavior in the Eocene causes the flow of high thermal magmatism influencing all Neo-Tethys subduction zones, such as East Iran and southern (Vincent et al., 2005; Ousta et al., 2024) Alborz (other than northern Alborz and Kopet Dagh). Due to the rollback of the downgoing oceanic plate in the Eocene and the removal of pressure, the melting lithosphere mantle and the asthenosphere rise. This asthenospheric uplift and the thinness of the crust produce large amounts of volcanic rocks in the Eocene of Alborz. The combination of these rocks often shows rare mantle elements (Verdel, 2009). However, studies and information on the origin of these volcanic activities are pretty limited. By considering the characteristics of the origin of these magmas, the current study presents a tectonomagmatic model for these magmatic activities.

Although this difference of opinion still exists in more recent studies, most researchers associate the formation of Cenozoic volcanic rocks with the subduction phenomena. For instance, Asiabanha and Foden (2012) proposed a back-arc rift basin for the Alborz area in the Eocene. According to Verdel (2009), the continuation of subduction with a shallow dip angle of the Neotethys oceanic lithosphere under central Iran might be responsible for the transfer of Oligo-Miocene magmatic activities from the Urmia-Dokhtar magmatic arc to the northern regions of central Iran and southern Alborz. Also, Alavi (1996) proposes an active continental margin magmatism model for Cenozoic volcanism. He claims that the Cenozoic magmatic belt of Western Alborz-Azerbaijan is a magmatic arc of the active continental margin. According to this researcher, this belt has been created by the subduction of the rift basin behind the Urmia-Dokhtar island arc beneath the Alborz subcontinent. This event has led to an arc-continent collision between the Urmia-Dokhtar island arc and the Alborz sub-continent. The border of this collision is considered to be in the northwest of Iran, corresponding to the North Tabriz fault. In this respect,

Haghnazar and Shafeie (2014) and Shafeie et al. (2016) believe that the Cenozoic magmatism in Alborz is associated with intracontinental rifts. According to these researchers, this magmatism is due to the magma produced by the 15% melting of a MORB mantle source with spinel composition. They also stated that partial contamination of this magma by continental crust rocks is such that they show false geochemical characteristics of subduction zone rocks.
Back-arc igneous activity occurred along an NW-SE arcuate belt ($> 1,200$ km long, Fig. 1 a) during the Late Cretaceous to Eocene, with the eruption of marine to subaerial magmatic rocks (Verdel, 2009).
The Tarom mountains, located in the northeast of Zanjan and adjacent to the Talesh mountains, form the southwestern end of the Alborz mountain range. They make a mountain range with a width of 60 km and an approximate NW-SE direction (Fig. 1). Some researchers (Berberian and King, 1981) consider Tarom a part of the Western Alborz. In contrast, (Ghorbani, 2013; Ashrafi et al., 2024) defined the Tarom region as the Tarom-Hashtjin subzone. They reported that this region lacks Paleozoic and Mesozoic bedrock, and its rocks are mainly igneous and pyroclastic with Cenozoic intrusive masses. According to previous studies in the Tarom Mountains, most of the volcanic rocks of the region erupted in the Eocene and belonged to the Karaj Formation. These studies have specified the Tarom magmatic zone in the structural zones of northern Iran along with the study area in the simplified tectonic map of Iran-Turkey (Asiabanha and Foden, 2012; Dabiri et al., 2018; Yazdi et al., 2019). The present study discusses different opinions about the tectonic setting of the rocks in the Tarom region as one of Iran's most important locations of Cenozoic magmatic activities.

2. Geology of Tarom region

The Tarom Mountains are part of the Alborz mountain range in the north of Iran and a part of the Alpine-Himalayan orogenic belt. These mountains are limited to the north by the Caspian Sea, to the south by the Central Iran zone, and the southwest by the Urmia-Dokhtar magmatic belt (Fig. 1) (Brunet et al., 2003; Zanchi et al., 2006). This region is a part of the Alborz-Azerbaijan range (Nabavi, 1976) and is located forming a part of the Tarom-Hashtjin range (Fig. 2). Although most researchers consider Tarom a part of the Western Alborz, (Ghorbani, 2013) introduced the Tarom region as the Tarom-Hashtjin sub-zone, which lacks Paleozoic-Mesozoic basement.
The Tarom Mountains zone, with a 60-km wide range and NW-SE trend, has a horst and graben structure (Lescuyer and Riou, 1976). In the Alborz-Azerbaijan area, the Eocene volcanic processes have generated some igneous rocks and marine lavas, known as the Karaj Formation in Iran's stratigraphy. These rocks are more than 2000 m thick (Dedual, 1967) with an age of middle Eocene (Ghorbani, 2013; Allen et al., 2003; Ghasempour et al., 2015). According to Hirayama et al. (1966), the rock outcrops of Tarom are mainly formed by pyroclastic deposits, lava flows, and Eocene sedimentary layers inside an antiform-shaped structure. Also, Ghorbani (2013) believes that the Tarom-Hashtjin subzone in the Cenozoic has a different geology from Alborz. In the Tarom zone, the rocks considered equivalent to the Karaj Formation in Alborz are lithologically and chemically different from those in Alborz. The formation of rocks in the Alamut region has been related to the magmatism of continental rift zones (Nazari Sarem et al., 2021).
The study area makes up a part of the northern slope of the Tarom range. The Tarom mountains mostly contain some igneous rocks extruded in to a shallow sea basin. Most of the volcanic rocks of the Tarom region erupted in the Eocene and belong to the Karaj Formation. Ryan et al. (1996) divide these lithological units into two members, Kordkand and Amand. The Amand Member, forming the upper part of the Karaj Formation, comprises sandstone, which begins and ends with a sequence of pyroclastic and magmatic rocks. In the study area, the Amand member has an extensive outcrop cut by granodiorite intrusive masses and Oligocene monzonitic quartz (Fig. 2). Tarom Neogene sediments (Fig. 2) outcrop along the Qezaluzen River in the core of a large-scale NW-SSE trend whose ridges are cut by faults (Hakimi Asiabar and Bagheriyan, 2018; Hakimi Asiabar et al., 2011). The region includes sandstone, mudstone, siltstone, conglomerate, and various colored marls. These units are mainly red and are equivalent to the Miocene red formations of Central Iran.

3. Study method

After field studies, thin sections were prepared from 50 rock samples of the region. Next, they were subjected to mineralogical and lithological characterizations using a polarizing microscope. For geochemical studies, 13 samples with the minimum alteration and weathering were selected and analyzed for major elements by inductively coupled plasma atomic emission spectroscopy (ICP-AES). Also, 13 samples were analyzed for trace elements and REEs by inductively coupled plasma mass spectrometry (ICP-MS) in the ACME laboratory in Toronto, Canada. The major and rare elements were measured by powdering the samples to pass through a sieve with a mesh size of 75 μm. To this end, 0.2 g of the sample is melted using lithium metaborate melting and dissolved by dilute nitric acid. Afterward, the values of the major elements were determined using the ICP-AES method, while the minor elements and REE were determined by the ICP-MS method. The analysis results of the main and secondary elements are shown in Table 1. Geochemistry and petrology diagrams were prepared using Igpet 2007 software using the results from the unaltered analyzed samples. Finally, they were used to investigate petrological processes, detect tectonic settings, and interpret them.

4. Petrography

The rocks of the study area are mainly composed of olivine basalt and olivine andesitic basalt. The dominant texture of the rocks is porphyritic with microlithic matrix to porphyritic with medium-grained matrix (Fig. 3). The texture of the medium-grained matrix in these basalts is attributed to the substantial thickness of the lavas. Accordingly, the slower cooling rate in the lower parts of the lavas has led to

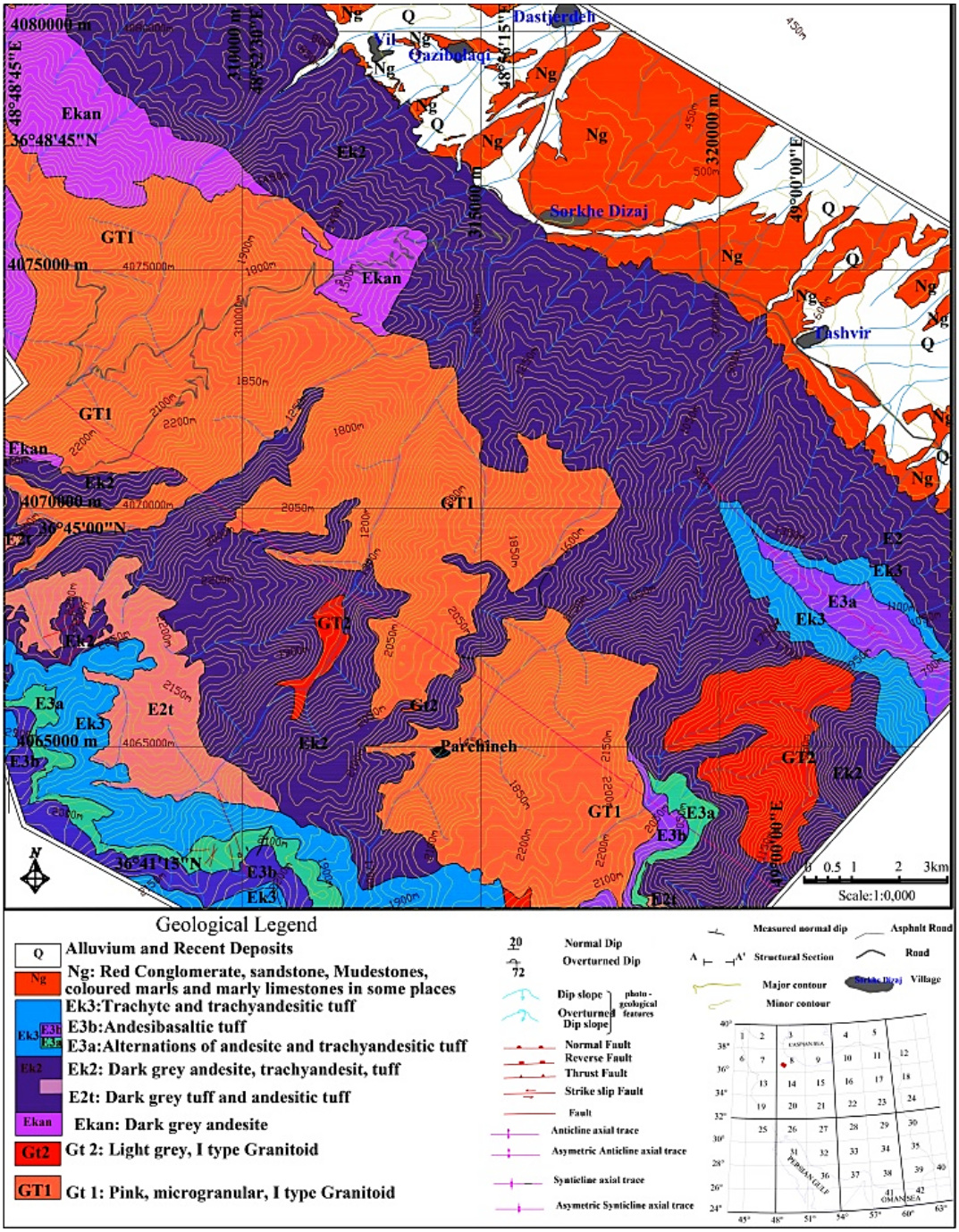

Figure 2. The 1:10:000 map of the study area; the range of this map is marked in Fig. 1 with a blue rectangle. All samples were taken from Ek2 and Ek3 rock units (Jamalomidi et al., 2022).

forming the medium-grained matrix in these basalts. The dominant phenocrysts of the rocks are clinopyroxene and olivine, in the order of their abundance. Clinopyroxenes are completely intact and euhedral with zoning structures. Olivine phenocrysts are fully altered to chlorite, iddingsite, and iron oxides (Fig. 3 b). Some olivines and apatite minerals are created in the poikilitic form, suggesting the priority of apatite crystallization over olivine and pyroxene. The matrix of these rocks is composed of plagioclase microlites, clinopyroxene grains (Fig. 3 d), and crystals of opaque minerals. One of the distinctive features of Tarom olivine basalts is the presence of carbonate fragments inside these rocks (Fig. 3 b). Therefore, they sometimes react with magma and completely transformed into fine clinopyroxene needles (Fig. 3 c). However, mica crystals are also occasionally seen in these rocks.

According to Mollo et al. (2010), the interaction of magma with carbonate minerals)calcite) in magma, Crystal fractionation causes the formation of a silica-undersaturated melt rich in alkaline elements. Experimental studies have shown that the absorption of carbonate in magma is accompanied by silica removal. This process leads to the formation of a solid solution consisting of diopside, hedenbergite, and the so-called Ca-Tschermark phenomenon (Mollo et al.,

Table 1. Results of experimental studies at different temperatures and combinations of water and carbonate (after Mollo et al. (2010)).

Run #	P (GPa)	T (°C)	Time (h)	Phases (wt.%)
1 wt.% H_2O				
2	0.5	1200	6	(1)Ol+(99)G
9	0.5	1150	24	(10)Ol + (44) Cpx + (1)Phl + (45)G
5 wt.% $CaCO_3$ + 1 wt.% H_2O				
14	0.5	1300	21	(100)G
16	0.5	1200	24	(8)Ol + (41)Cpx + (1) Phl+(50)G
8	0.5	1150	24	(9)Ol + (66) Cpx + (1)Phl+(29)G
10 wt.% $CaCO_3$ + 5 wt.% H_2O				
13	0.5	1300	6	(100)G
15	0.5	1200	24	(5)Ol + (50)Cpx + (1) Phl +(44)G
12	0.5	1150	23	(4)Ol + (60) Cpx + (1)Phl + (30)G
20 wt.% $CaCO_3$ + 5 wt.% H_2O				
10	0.5	1300	15	(100)G
5	0.5	1200	24	(3)Ol + (56)Cpx + (1) Phl + (40)G
7	0.5	1150	24	(1)Ol + (75) Cpx + (1)Phl + (22)G
10 wt.% $CaCO_3$ + 5 wt.% H_2O				
24	0.5	1150	11	(14) Phl + (4)Ol + (20)Cpx + (62)G
10 wt.% $CaMg(CO_3)_2$ + 5 wt.% H_2O				
23	0.5	1150	11	(15)Ol + (51) Cpx + (1)Phl + (33)G

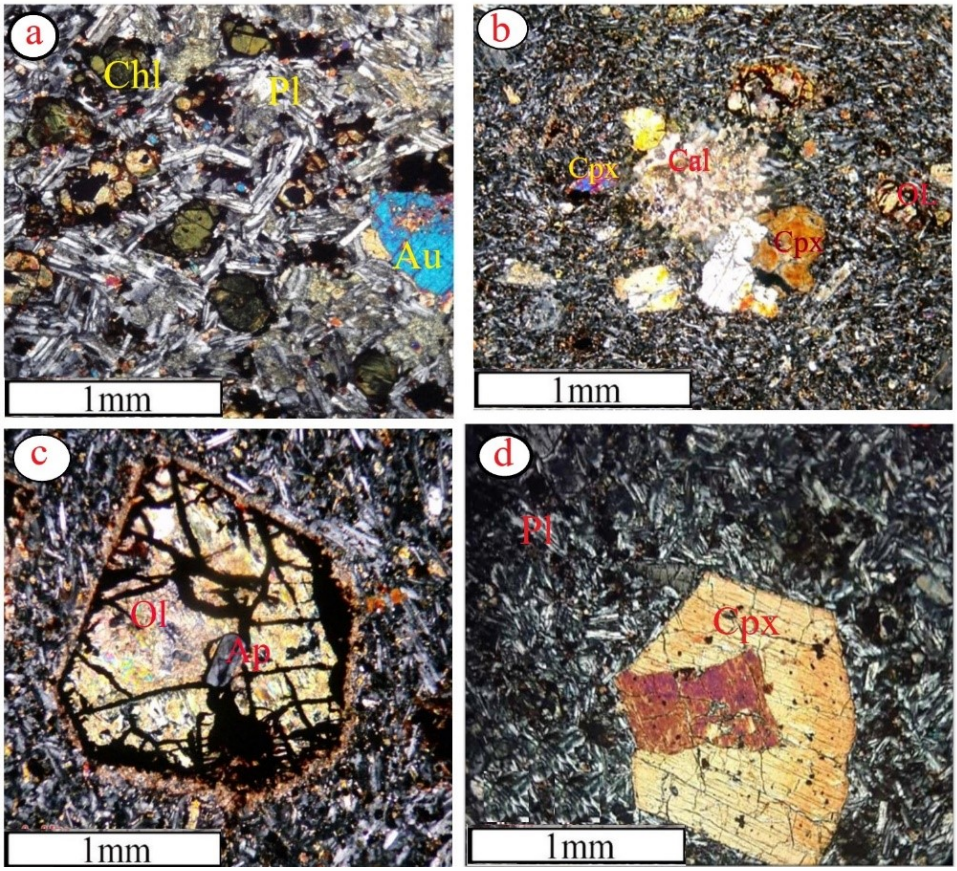

Figure 3. a-a view of pyroxene and plagioclase Phenocrysts in olivine basalt under XPL. b- assimilation of carbonate minerals by olivine basalt magma, a part of which turned into pyroxene needles (under XPL). c- olivine phenocryst enclosing apatite crystal (under PPL). d- clinopyroxene phenocryst in olivine andesitic basalt. Pl = plagioclase, Ol= Olivine, Opq= opaque minerals, chl=chlorite. Ap= apatite, Au= augite, Whitney and Evans (2010).

2010). This process is characterized by the disintegration of $CaCO_3$ in the melt and the consumption of SiO_2 and MgO to form diopside. The chemical formulation of this reaction is as follows:

$$CaCO_3^{Solid} + SiO_2^{Melt} + MgO^{Melt} \longrightarrow Diopside^{Solid} + CO_2^{Fluid}$$

According to this reaction, the amount of carbonate absorption is controlled by the amount of MgO present in the melt. Although this reaction may apply to early basaltic magma, it certainly did not occur in intermediate composition and evolved magma systems (Barnes et al., 2005; Mollo et al., 2010). The experimental results of this study show that in a system containing $CaCO_3$, the amount of Ca-Tschermak and hedenbergite increases with increasing the $CaCO_3$ concentration, while the amount of diopside remains constant (Fig. 4). Accordingly, the reaction produces silica-undersaturated melts (Fig. 4) in which a magnesium solid solution forms clinopyroxene (Al, Fe, and Mg) instead of diopside (Fig. 5). The figure (Fig. 5) presents Ca-Tschermak (CaTs), hedenbergite (Hd), and diopside (Di) studied at 1200 and 1150 °C and with different amounts of $CaCO_3$. With increasing the amount of $CaCO_3$ and the decreasing temperature, the molar mass of CaT and Hd increases. As a result, the absorption and fractional crystallization vectors coincide. Besides, the molar amount of diopside remains almost constant during the increase in $CaCO_3$ concentration, while its weight percentage increases due to the temperature decline. Therefore, absorption and reduction crystallization vectors follow different directions (Fig. 5).

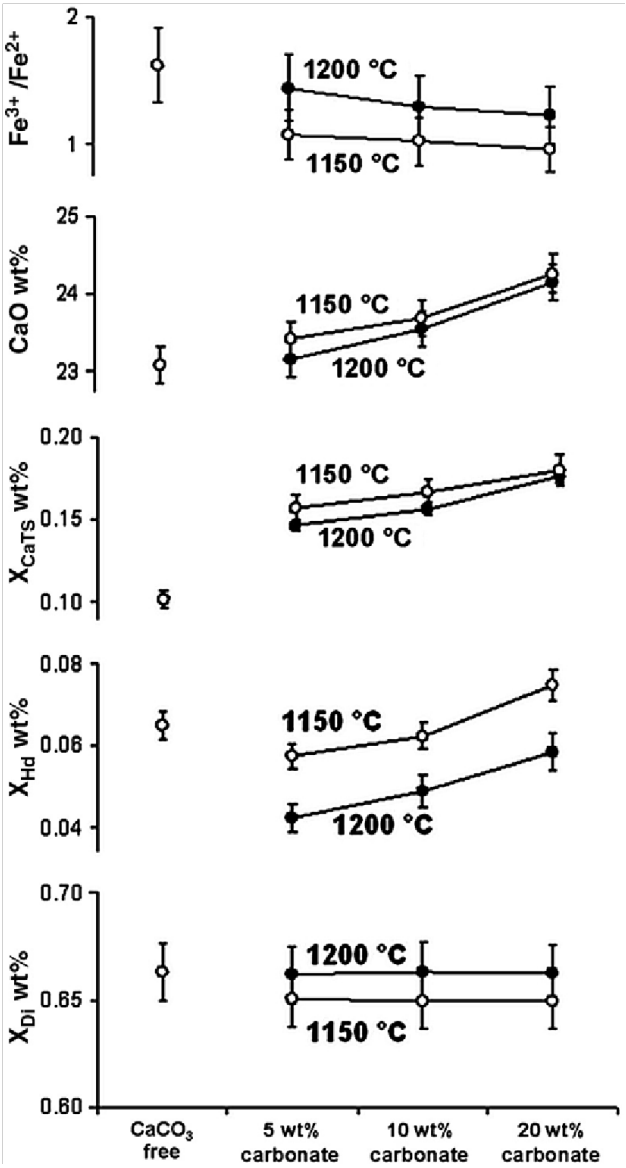

Figure 4. Clinopyroxene compositional changes in the presence of free $CaCO_3$ and experimental $CaCO_3$-bearing compounds (Mollo et al., 2010).

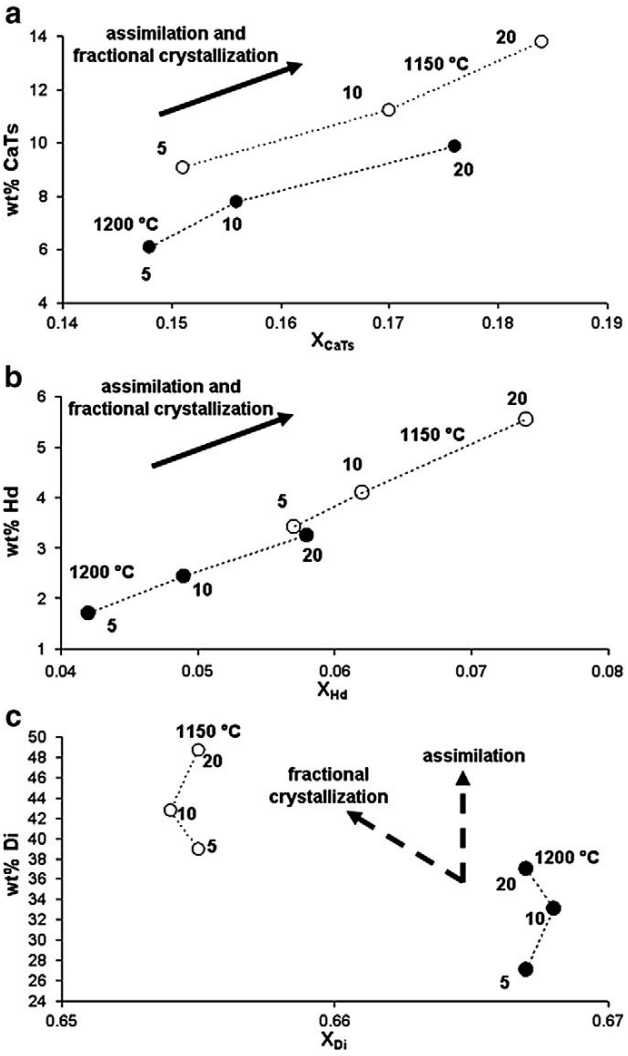

Figure 5. Wt.% components of experimental clinopyroxene plotted versus respective molarfraction. The mass is calculated as follows: total amount of clinopyroxene (in wt.%, Table 1) times molar fraction of Ca-Tschermak, hedenbergite, and diopside component (Table 2). a-Ca-Tschermak (CaTs) vs. XCaTs. b-Hedenbergite (Hd) vs. XHd. c-Diopside (Di) vs. XDi. Numbers (5, 10, and 20) in the figure refer to the wt.% of $CaCO_3$ added to the charge (after Mollo et al. (2010)).

It is of note that in some areas (e.g., East Africa), the assimilation of lime (as sedimentary calcareous xenoliths) was proposed to produce alkaline feldspathoid rocks (Mollo et al., 2010). However, later REE studies revealed that these fragments are indeed intrusive carbonates (Middlemost, 1975). Experimental studies have shown that the reactions involving carbonate contamination are more complicated than before. Carbonate contamination is a three-phase process (i.e.,

solid, melt, and liquid) with the following main products: 1) a solid solution of clinopyroxene (diopside-hedenbergite-Ca-Tschermak), 2) a melt rich in CaO and undersaturated with silica, and 3) a fluid C-O-H phase. Magma contamination with carbonates affects mineral textures, compositional balance, and chemistry. These effects are as follows:

1. Nucleation in clinopyroxenes is more than in olivines.
2. The growth of olivines is more than pyroxenes.
3. Clinopyroxene is mostly Hedenbergite and Ca-Tschermak type.
4. The amount of molten silica is reduced, thereby having a direct effect on the distribution of Mg-Fe^{2+} between the melt and olivine.
5. Fayalite concentration in olivine and the Fe^{+3}/Fe^{+2} ratio in clinopyroxenes change with increasing fO_2 in a closed system. This issue should be considered when studying carbonatite magmas and magmatic skarn (Mollo et al., 2010).

In some experimental studies on melt and the carbonate wall rock, Mollo et al. (2010) showed that the amount of clinopyroxene increases with increasing the carbonate content, even at a constant temperature (Table 1).

5. Geochemistry

Table 2 presents the results of the main and secondary elements. In the diagram of total alkaline versus SiO_2 from Cox et al. (1979), all samples fall in the basalt field and the alkaline magmatic series (Fig. 6 c). Also, in the diagram of SiO_2 versus Zr/Ti by Winchester and Floyd (1977), all samples fall in the range of alkaline basalts (Fig. 6 a). Since $K_2O.Na_2O$ ratio is equal to 1 on average, they are placed in the potassium alkaline series (Fig. 6 d) according to the classification by Middlemost (1975). In weight norm calculations, olivine was calculated along with nepheline, whose nepheline concentration is less than 5%. Therefore, according to the classification by Yoder and Tilley (1962), they are considered alkaline olivine basalts. The Mg# in the samples varies between 5.55 and 5.46, indicating the transformation of alkaline olivine basalts in the region. In the plat of SiO_2 changes against Mg#, a decrease in SiO_2 concentration is seen along with a decrease in Mg# and an increase in fractional crystallization (Fig. 6 b). This result suggests that after the assimilation of carbonate rocks by magma, Si and Mg were consumed to make clinopyroxene in magma. Thus, with further evolution, the amount of these two elements declined in the remaining magma.

In diagrams normalized to chondrites and primitive mantle (Sun and McDonough, 1989) REE and trace element distribution patterns of samples show positive anomaly trends in large-ion lithophile elements (LILEs), light and medium REEs (LREEs and MREEs), Nb, and Ta—elements related to alkaline within plate magmatism and similar to enriched mantle (McDonough and Frey, 1989) rock (Fig. 7 a and b). Comparison of the normalized pattern of trace elements of Tarom olivine basalts with the values of MORB composition given by Pearce (1983) and primary mantle composition proposed by Holm (1985) revealed a distinct enrichment in LILEs, along with positive anomalies of Ce, P, and Sm and negative anomalies of Nb, Ta, Zr, Hf, and Th. The pattern of trace elements of Tarom basalts normalized with values Pearce (1983) and primary mantle values Holm (1985) are shown in Figs. 7 c and 7 d. Enrichment of LIL elements along with positive anomalies of Ce, P, and Sm and negative anomalies of Nb, Ta, Zr, Hf, and Th are observed. One of the most obvious features of spider diagrams of subduction basalts is a distinct depression in Nb-Ta. However, according to Wilson (1989), this type of depletion is also observed in the spider diagrams of intercontinental basalts contaminated with continental crust. Therefore, in his opinion, one should be careful in the interpretation of these patterns. Such patterns observed in normalization diagrams are characteristic of spider diagrams of subduction zones (Wilson, 1989; Pearce, 1982) and have also been reported in intercontinental basalts (continental rift basalts and continental flood basalts) (Cox and Hawkesworth, 1985; Wilson, 1989). According to many researchers, the negative anomalies of Ti, Zr, Ta, and Nb and the positive anomaly of K are indicators of contamination of magmas with the continental crust (Hoffman, 1997; Wilson, 1989; Taylor and McLennan, 1985).

According to the obtained elemental proportions, the following comparisons can be made.

1. K_2O/P_2O_5 in alkali olivine basalts of the studied range located on the northern slopes of Tarom Mountains is 5.6 on average. Typically, basalts originating from the mantle have $K_2O.P_2O_5 \leq 2$ (Carlson, 1991). This ratio increases due to crustal assimilation or crystalline differentiation of apatite. This issue has also been observed in Columbia River basalts (in the western United States).
2. Nb/U in alkali olivine basalts of the region is 8.8 on average. This ratio is 47 ± 10 in MORB and OIB source basalts (Hofmann et al., 1986), 30 in the primary mantle, and 10 in the continental crust (Hoffman, 1997). If the continental crust is responsible for magma contamination, the Nb/U ratio will decline.
3. The average La/Nb in the alkali olivine of Tarom basalts is around 3, less than 1 in continental alkaline basalts of OIB origin, and between 0.5 and 7 in some provinces of continental basalts that show variable degrees of crustal contamination. (Thompson et al., 1984). Since the La/Nb is greater than 1 in the crust, the contamination of the basalt crust leads to an increase in this ratio (Taylor and McLennan, 1985).
4. The magmas originating from the mantle have a Th.Ce of about $0.02 - 0.05$ (Sun and McDonough, 1989). A high Th/Ce ratio is strong evidence for crustal contamination of magma (Su et al., 2012). Th. Ce is 0.15 in the upper continental crust (Taylor and McLennan, 1985) and 0.06 in the lower crust (Rudnick and Fountain, 1995). This ratio is about 0.06 in the basalts of Dizaj-Dastjerdeh, which signifies magma contamination with the lower crust.

Table 2. Chemical analysis of main elements by ICP-AES method in terms of weight percentage and secondary elements by ICP-MS method in terms of PPM.

Sample (major elements)	M212	M211	M209	M208	M207	M204	M203	M202	M201	M200	M199	M198	M197
SiO_2	46.94	47.10	45.76	47.74	47.55	45.54	48.21	47.73	48.87	47.32	48.79	49.05	49.61
Al_2O_3	16.44	16.25	16.58	15.88	16.37	14.82	16.10	15.43	15.65	15.96	15.94	15.68	17.13
Fe_2O_3	11.33	11.61	11.74	11.04	11.30	11.04	11.46	10.95	10.14	9.75	10.11	9.88	9.08
MgO	5.22	5.73	5.14	6.11	5.59	5.78	6.73	6.84	6.10	4.72	6.02	6.05	3.94
CaO	10.04	9.35	9.52	9.25	9.24	11.21	9.63	10.05	10.71	9.96	10.68	10.28	8.57
Na_2O	2.32	2.33	2.30	2.39	2.44	2.06	2.48	2.29	2.46	2.42	2.48	2.47	2.31
K_2O	2.33	2.51	2.95	2.57	2.60	2.40	2.71	2.40	2.39	2.27	2.27	2.51	3.14
TiO_2	1.04	1.04	1.03	0.97	1.02	0.94	0.97	0.95	0.93	0.94	0.94	0.94	0.93
P_2O_5	0.38	0.38	0.39	0.41	0.39	0.40	0.44	0.39	0.35	0.35	0.35	0.35	0.45
MnO	0.15	0.18	0.14	0.21	0.17	0.19	0.21	0.19	0.16	0.20	0.16	0.15	0.20
Cr_2O_3	0.011	0.014	0.013	0.025	0.018	0.026	0.025	0.032	0.020	0.020	0.021	0.023	0.007
Mg#	48.05	49.43	46.45	52.31	49.50	50.92	53.77	55.32	55.55	47.82	53.84	55.55	45
LOI	3.5	3.2	4.1	3.0	3.0	4.9	0.7	2.4	1.9	4.6	2.0	2.3	4.3
Sample (minor elements)	M212	M211	M209	M208	M207	M204	M203	M202	M201	M200	M199	M198	M197
Ni	20	35	28	30	22	39	38	45	40	31	35	45	20
Sc	32	31	31	30	30	32	30	33	33	32	33	33	19
Ba	514	549	557	557	556	535	615	573	508	507	493	522	1335
Co	35.2	36.2	31.5	35.1	34.5	38.6	37.8	36.2	33.3	34.5	32.0	32.0	25.6
Cs	0.8	1.1	1.0	0.7	0.5	1.0	2.0	3.2	10.3	4.7	6.3	3.6	6.5
Hf	1.9	2.3	2.0	2.7	2.2	2.2	2.8	2.6	2.8	2.1	2.4	2.6	3.1
Nb	7.7	6.5	6.2	5.8	6.1	5.2	5.8	5.5	5.4	5.4	5.4	6.6	7.7
Rb	43.5	47.0	57.2	52.1	51.3	45.6	50.8	48.9	53.7	51.6	50.2	56.6	59.1
Sr	687.7	730.1	678.5	757.8	698.0	980.0	827.1	792.2	723.0	637.1	669.9	656.2	784.4
Ta	0.4	0.3	0.3	0.3	0.3	0.2	0.3	0.2	0.3	0.2	0.2	0.3	0.5
Th	1.9	2.0	2.0	2.2	1.9	1.9	2.3	1.9	2.7	3.1	2.8	3.7	3.7
U	0.6	0.6	0.5	0.9	0.7	0.7	0.9	0.6	0.9	1.1	0.9	1.2	1.1
V	301	299	298	288	292	278	289	294	293	310	289	274	232
Zr	78.8	80.9	82.3	83.9	83.3	78.6	87.6	84.6	98.2	95.1	94.0	104.9	141.2
Y	20.9	21.7	21.6	21.8	21.2	19.4	21.2	20.9	20.8	20.0	20.1	21.6	23.1
La	17.0	17.7	17.9	18.7	18.4	18.0	19.8	18.9	18.4	19.2	19.0	20.7	24.9
Ce	35.1	35.2	36.2	38.7	38.0	36.8	41.4	39.6	37.1	37.1	37.9	41.1	49.4
Pr	4.44	4.55	4.70	4.85	4.89	4.85	5.14	4.92	4.81	4.96	4.84	5.26	6.13
Nd	20.4	19.2	19.0	20.8	20.6	19.8	21.8	20.9	20.0	21.1	21.3	21.5	23.9
Sm	4.62	4.87	4.53	4.61	4.25	4.47	4.50	4.65	4.46	4.36	4.31	4.83	5.23
Eu	1.39	1.34	1.45	1.30	1.38	1.37	1.44	1.36	1.43	1.33	1.39	1.45	1.58
Gd	4.88	4.95	4.59	4.66	4.38	4.33	4.67	4.66	4.46	4.25	4.27	4.76	4.74
Tb	0.68	0.68	0.66	0.64	0.65	0.64	0.65	0.64	0.64	0.62	0.63	0.68	0.69
Dy	4.39	3.66	3.60	3.97	3.93	3.61	3.93	3.72	3.65	4.10	3.83	3.81	4.10
Ho	0.72	0.83	0.78	0.70	0.73	0.69	0.71	0.72	0.75	0.73	0.75	0.80	0.77
Er	2.16	2.23	2.21	2.01	2.28	1.88	2.12	2.11	1.78	2.15	2.11	2.16	2.22
Tm	0.35	0.30	0.32	0.30	0.31	0.28	.30	0.28	0.29	0.31	0.29	0.31	0.31
Yb	1.90	2.08	2.04	2.28	1.82	1.87	1.82	2.04	1.91	1.90	1.89	2.24	2.13
Lu	0.29	0.31	0.33	0.30	0.31	0.26	0.30	0.29	0.29	0.28	0.30	0.31	0.30
Cu	52.1	120.6	40.6	239.8	191.5	96.5	72.7	150.7	252.0	9752.5	55.1	52.9	36.4
Pb	169.7	222.2	124.5	691.3	101.0	3648.1	39.6	371.5	530.5	156.3	129.9	221.2	295.7
Zn	84	63	71	68	54	56	72	65	36	91	34	28	77

5. Comparing the pattern of alkaline rare earth elements in olivine basalts of the Amand member in Tarom in the Tashevir area with the normalized values of the lower crust (Fig. 8 a and 8 b), the primary mantle, and MORB shows the harmony of the elemental trend of basalts in the area with the lower crust. A negative Th anomaly is observed in the alkali olivine basalts of the study area. Magma contamination with the granulitic facies of the lower crust causes depletion of Nb-Ta and U-Th elements in the lower crust compared to the LREE (Borisova et al., 2001). Typically, the active role of subduction components and fluids, on the one hand, and the contamination of the lower crust with the upper continental crust, on the other hand, increase Th concentration (Pearce, 1983; Farahat et al., 2006).

According to Mason and Moore (1982), the dehydration of the subducting plate caused the metasomatism of the upper mantle wedge by aqueous fluids. As a result, it caused the positive anomaly of Rb and K and the negative anomaly of Ba in the magma. In contrast, in the samples of the study area, which includes the uppermost part of the Karaj Formation, a positive anomaly of Ba and a negative anomaly of Rb are observed. Thus, the role of subduction fluids and the upper crust in magma evolution is doubted. The same enrichment and depletions and the harmony of the elemental trends of the basalts of the region with the underlying continental crust indicate the contamination of these rocks with the lower continental crust. Other studies (Turner and Hawkesworth, 1995) also indicate that magma contamination with the lower crust can affect some continental basalts. The studied samples indicate similarity with the enriched back-arc basalts and their difference with the island arc basalts, which have a negative correlation between Ba/Nb and Ba/Yb (Li et al., 2013) (Fig. 9). Since Zr and Nb behave in an incompatible fashion during fractional crystallization of olivine, pyroxene, magnetite, and plagioclase in basaltic magmas, they are suitable representatives for the composition of the source site (Reichow et al., 2005). The K and Ba are generally used to identify the addition of fluids in a magma source and the Th and La are less affected by the fluids. Therefore, the ratios of Ba/Th and Ba/La are effective indicators with a variable range for fluid addition in the magma origin (Sun et al., 2022). The Zr/Nb ratios of the volcanic rocks of the region (5 – 10)((Fig. 9 c) are in the continental rift range, and this ratio was lower than the continental crust (16.2) in the OIB mantle sources. (14.8), and normalized-MORB (N-MORB) (30) (Saunders et al., 1988; Weaver, 1991). Here, Sm is incompatible with Yb in the mantle. Also, because it exists in the pyroxene structure and, if present, in the amphibole structure, its concentration compared to Yb varies sharply during the melting processes in the mantle (Li and Che 2014). The diagram of the samples studied in the Mohr and Kampunzu (1991) diagram, placed in the continental rifts (Fig. 9 c) and in the

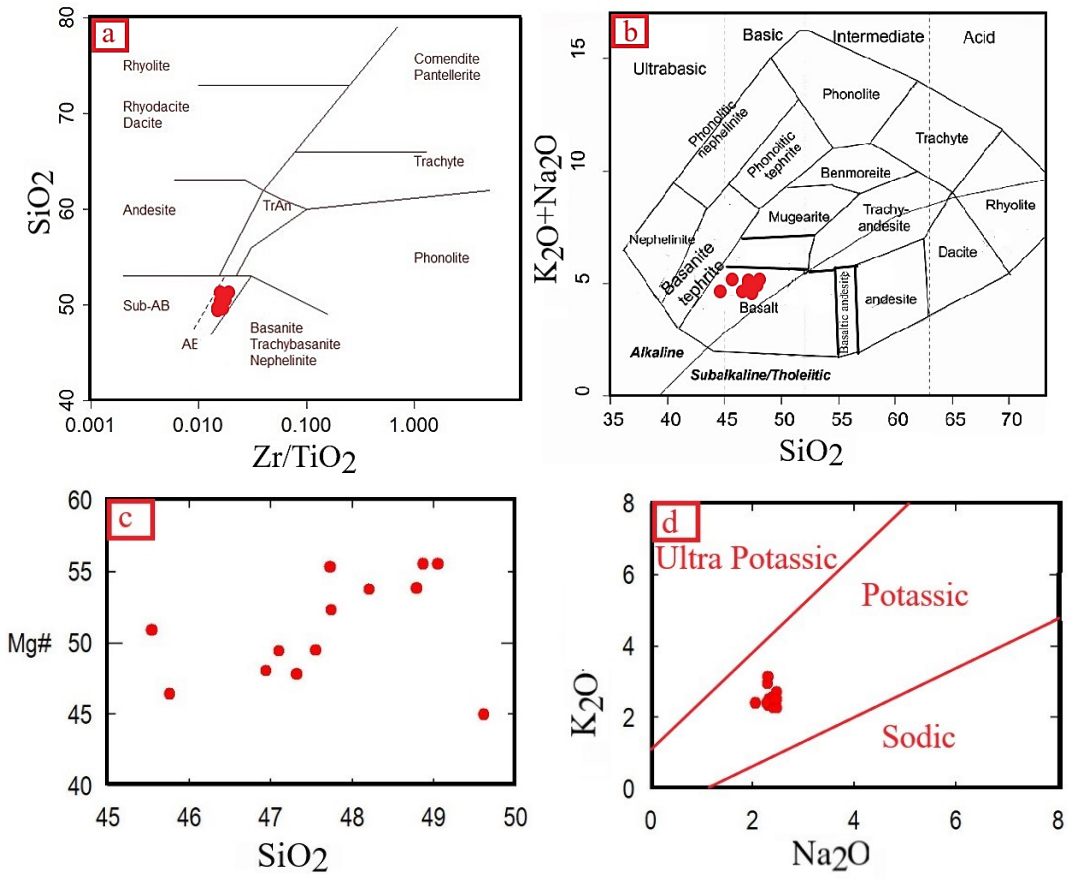

Figure 6. a-Division of regional rocks in the diagram of SiO_2 against Zr/TiO_2 (Winchester and Floyd, 1977). b-the position of the samples in the diagram of Cox et al. (1979). c-the position of the samples on the graph of SiO_2 versus Mg# (Winchester and Floyd, 1977). d-the position of the samples in the diagram of Middlemost (1975).

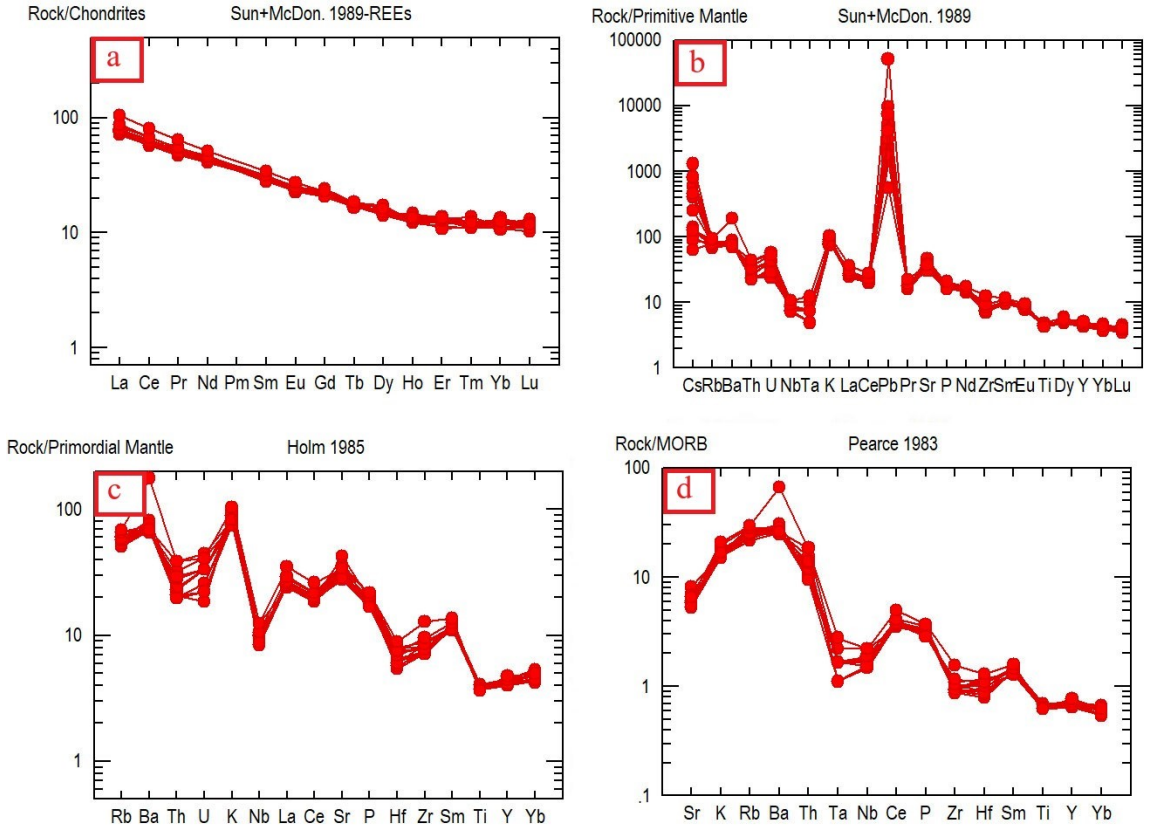

Figure 7. a-The trace element pattern of Tarom olivine basalts normalized to Chondrites composition (Sun and McDonough, 1989). b- Primordial Mantle composition (Sun and McDonough, 1989). c- Primordial Mantle composition (Holm, 1985). d-MORB composition (Pearce, 1983).

diagram Kamenov et al. (2004), which depicts the basalt ocean (NMORB, EMORB, and OIB) and continental crust, are in the area of the crust (Fig. 9 d).

6. Discussion

6.1 Input components from the oceanic crust to the origin site during subduction

The selective enrichment of LILE and the LREE along with the positive Pb anomaly in the studied samples (Fig. 10) can be explained by the involvement of components derived from the subducting oceanic plate or partial melting of the oceanic crust at the source (Keskin et al., 1998). Fluids and melting released from the melting of the oceanic crust sediments are usually considered in the subduction zones of two important factors. The mobility of elements in components derived from the subducting slab in the subduction zone is investigated comparatively. For instance, Ba, as a LILE, is soluble in fluids and has higher mobility than the elements of the REE group. As a result, adding fluids released from the oceanic plate to the mantle wedge raises the Ba/La ratio. In comparison, in melts derived from plate sediments, the

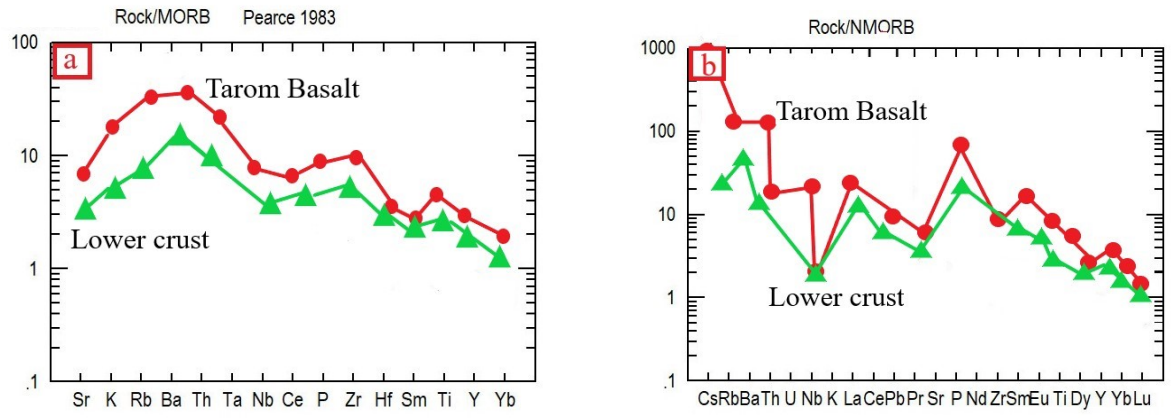

Figure 8. The pattern of average alkaline trace elements of olivine basalts of the Tarom range compared to normalized lower crust values with a) MORB values and b) NMORB values.

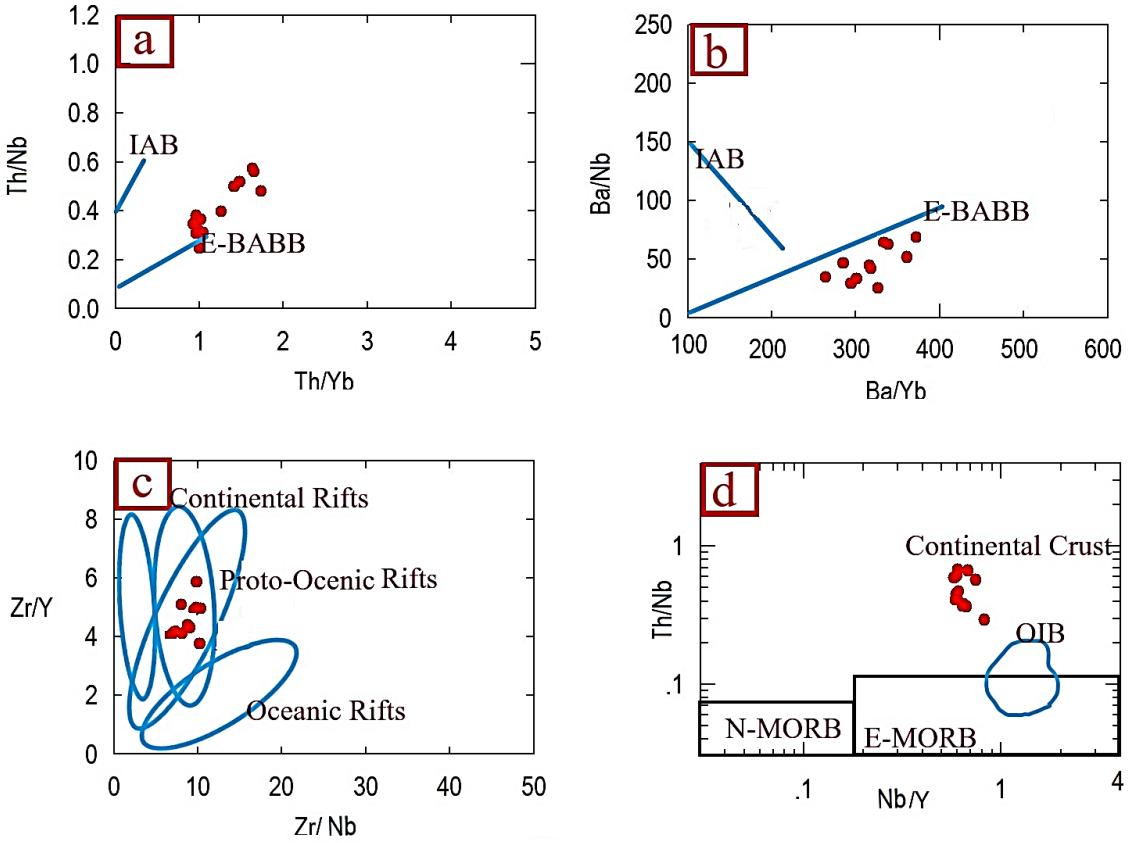

Figure 9. a and b-diagrams of Li et al. (2013). c- diagram of Kampunzu and Mohr (1991). d-diagram of Kamenov et al. (2004).

Th/Yb remains constant due to the immobility of Th and Yb in fluids (Woodhead et al., 2001). Therefore, elemental ratios such as Ba/La and Th/HREE are considered useful tracers of fluid or sediment involvement in the evolution of subducting magmas. Basalt samples of the study area, regarding the variable Ba/La values and almost constant Th/Yb (Fig. 9 a), indicate an origin enriched by fluids derived from the oceanic slab and, to some extent, melts from sediments before melting. The negative anomaly of Nb and Ta (often Nb/Ta < 1.8) may be due to alteration caused by fluids released from the oceanic crust. These results are confirmed by the LILE enrichment in the samples. In this respect, the low ratios of La/Yb (0.12) and Nb/Y (3.3) show that the enrichment of the source area was created by fluids released from the subducting oceanic plate (Hoffer et al., 2008). In the diagram of Nb/Yb versus Th/Yb (Pearce, 1983), the studied samples are placed on the top of the mantle range. Therefore, it is inferred that their parent magma has a mantle origin relatively enriched by subduction components. Our samples have slightly variable Nb/Y ratios, showing a trend of fluid-related metasomatism in Fig. 10d and such characteristics could be interpreted as derivation from a subduction-modified source.

6.2 Mantle origin and tectonic environment

The Late Cretaceous-Paleogene arc magmatism in Iran accompanied strong extension and lithospheric thinning— in the overlying plate of the subduction system- including in the back-arc environment (Shafaii Moghadam et al., 2020). Paleogene Iran may be considered as a type example of an extensional continental convergent margin. The lithospheric extension is likely to lead to further weakening induced by the upwelling of the hot asthenosphere, and this will help further rifting of the convergent margin (DeCelles et al., 2009; Ducea et al., 2015; Ferrari et al., 2013; Seebeck et al., 2014). Convergent margin rifting can be caused by trench retreat, slab roll-back, steepening slab tearing, or lithospheric delamination. We suggest that extension in the Iranian plateau triggered both lithospheric and asthenosphere mantle upwelling beneath the Back arc and generated different types of magmas (Sepidbar et al., 2019), but the asthenospheric mantle contributed extensively to the genesis of Late Cretaceous magmatic rocks because these rocks have more juvenile or depleted isotopic signatures. On the other hand, Eocene extension and crustal thinning were accompanied by decompression melting of the pre-existing mantle wedge as well as incorporating underlying upwelling asthenosphere (Shafaii Moghadam et al., 2020). Continental basalts have a wide diversity such that their origin has been among the subjects of petrology in recent decades. The compositional changes of basalts in the continental basins indicate the high potential of the interaction between the lithosphere and the magma rising to the earth's surface. This issue can be proven by comparing the range of chemical and isotopic compositions of the intercontinental basalts and oceanic basalts (Carlson, 1991). However, understanding the origin of magma and the related tectonic environment in continental environments is generally diffi-

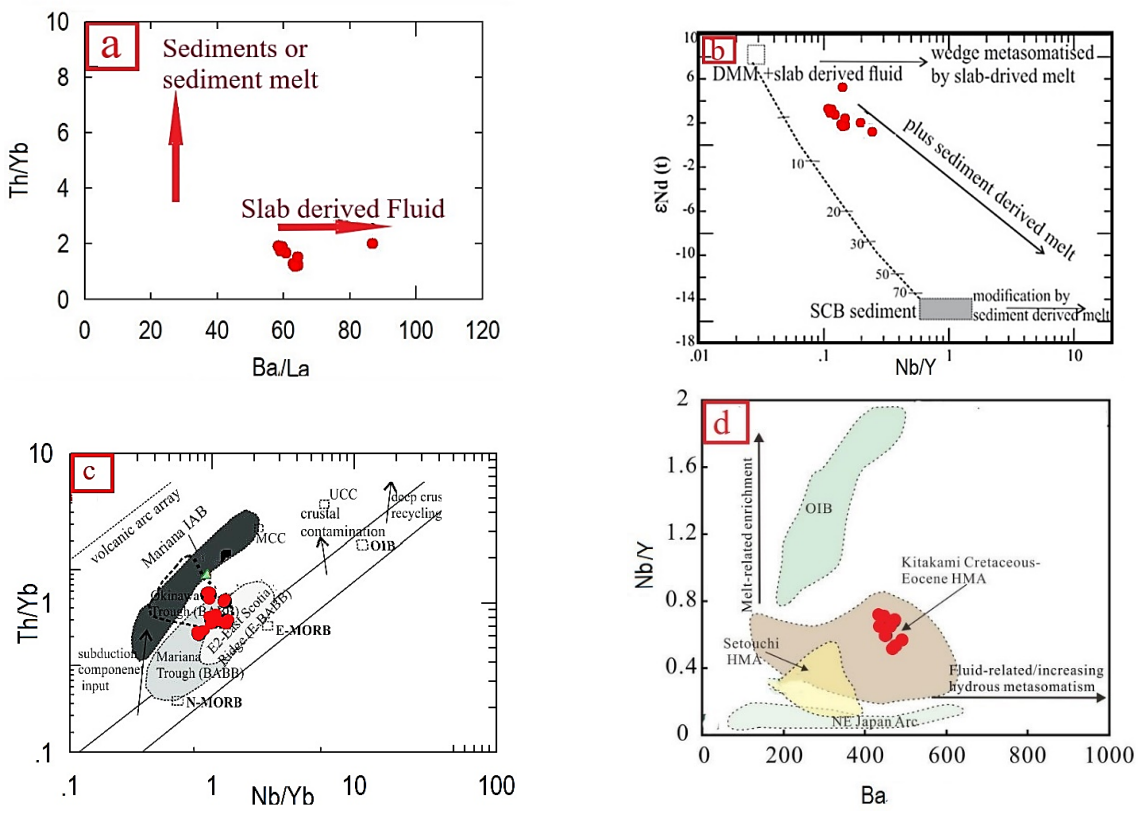

Figure 10. a- Ba/La vs. Th/Nb plot of Wang et al. (2010). b- Nb/Y vs. £ Nd plot of Wang et al. (2013). c- Nb/Yb vs. Th/Yb plot of (Pearce, 2008). D- Ba vs Nb/Y diagram (after Zhang et al. (2022)).

cult. For this purpose, it is necessary to study the history of magmatic evaluations while passing through the lithospheric mantle and continental crust. In this regard, since continental crust can have chemical signatures similar to subduction zones (Verma, 2009), it can hide mantle signs. The Ba/Rb in the basalts of the study area is around 11.5 on average. Generally, the sediments and fluids released from the subducted slab have a low Ba/Rb due to the more mobile Rb over Ba in the subducted solutions (Tatsumi et al., 1986; Peccerillo, 1999). This ratio is about 11 in non-orogenic basalts (Sun and McDonough, 1989). On the other hand, K_2O/Na_2O in olivine basalts of the region is almost equal to 1 Usually, magmas associated with orogenic areas have a ratio of $K_2O/Na_2O > 1.5$ (Willson and Downes, 2006). Therefore, K_2O/Na_2O and Ba/Rb in the olivine basalts of the study area indicate that these rocks are associated with non-orogenic areas.

Fig. 8 (a) presents the position of the samples in the Zr/Nb versus Y/Nb diagram from Wilson (1989). This diagram, which demonstrates a trend that is a mixture of an enriched MORB (E-MORB) source and the lower continental crust, follows the crustal contamination vector. In addition, the position of the samples in the diagram of Ba/La versus La/Sm from Ryan et al. (1996) indicates that they have constant Ba/La values and follow the crustal contamination trend (Fig. 11). This result indicates the lack of involvement of a subduction-induced fluid phase in the petrogenesis of rocks in the region. According to Wilson (1989), this trend indicates the involvement of the MORB asthenospheric mantle source in the petrogenesis of alkaline olivine basalts.

In the diagram of Zr/Y vs Zr from Pearce (1983), the samples are located in the typical range of MORB and intercontinental basalts (Fig. 8 c). Crustal contamination in studied rocks has decreased Zr concentrations leading to a negative Zr anomaly. In this respect, the original uncontaminated samples might have a higher Zr content. Thus, the real tectonic setting of the samples is intercontinental. The trend of magmatic evolutions was determined using the parameter ΔNb (Eq. (1)) introduced by (Fitton et al., 1997):

$$\Delta Nb = [1.74 + \log(\frac{Nb}{Y}) - 1.92\log(\frac{Zr}{Y})] \qquad (1)$$

The logarithmic diagram (Fig. 11 d) of Condie (2005) is drawn based on these trends. This diagram is generally insensitive to the alteration effects, crystalline differentiation, and variable degrees of partial melting. Overall, it is used to characterize the magma source area and separate plume and non-plume basaltic sources. In this diagram, basalts related to subduction, N-MORB, and continental crust are located in the lower part of the line; i.e., ΔNb is less than zero for these basalts (Condie, 2005). In the logarithmic diagram of Nb/Y against Zr/Y, the samples of the study area have $\Delta Nb > 1$. Therefore, they are located near the boundary of the source and origin of the plume and are not related to arc areas (Fig. 10 d). Crustal contamination of a basalt originating from a depleted source or a subduction zone or N-MORB cannot cause a positive anomaly. However, if basalts of ocean island basalt (OIB) source or plume origin are contaminated with continental crust, it will cause a negative ΔNb in the samples (Condie, 2005) The crustal

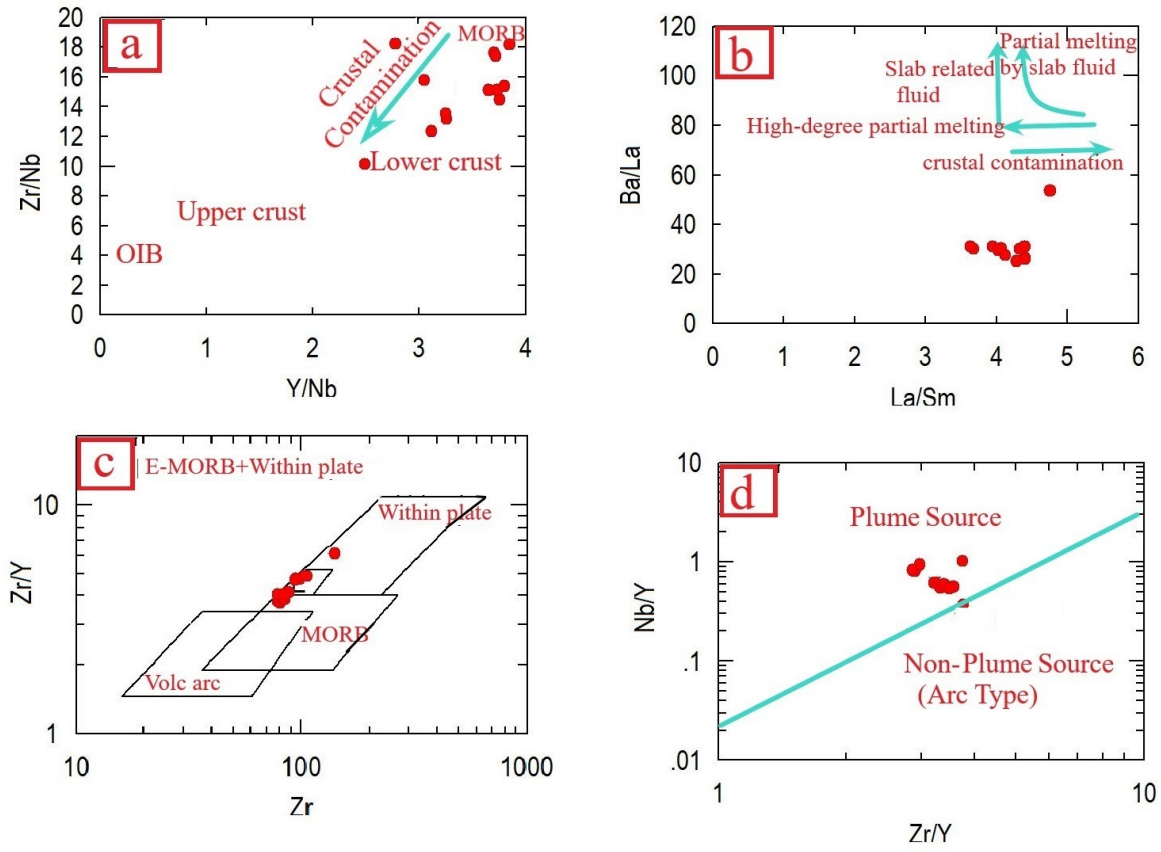

Figure 11. a- the location of samples in the Zr/Nb versus Y/Nb diagram from Wilson (1989). b- the location of samples in the Ba/La versus La/Sm diagram from Ryan et al. (1996); c- the location of the samples in the diagram of Zr/Y versus Zr from Pearce (1983). d- the position of the samples in the logarithmic plot of Nb/Y against Zr/Y from Condie (2005).

contamination in the basalts of the study area and the ΔNb > 0 in the samples suggest that the basalts in the Tashevir region have a plume origin has rather Been derived from melting of N-MORB or having an active continental margin setting (Shuqing et al., 2003), all the samples of the study area are located in the IV2 area, i.e., intercontinental basalts and continental rift zone basalts (Fig. 12 a). In the diagram of Nb/Ta against Zr/Sm (Fig. 12 b) by Foley et al. (2003), the samples also show a trend from a mantle MORB source toward continental basalts. The magmatic series of volcanic and plutonic rocks of the study area are calc-alkaline with high potassium and are enriched with elements such as Th, Sr, Ba, Rb, and K. Their textural and mineralogical characteristics of these rock series indicate the presence of water-rich vapor phase in their producing magma.
According to (Kurt et al., 2008), the Nb-Ta depletion and LILE and LREE enrichment can be caused by two factors:

a) The origin of magmas from a mantle enriched by subduction fluids

b) Crustal contamination of magma originating from the mantle

Previous geochemical studies addressed the involvement of the MORB source asthenospheric mantle and lower continental crust in the petrogenesis of alkaline olivine basalts in the intercontinental basin. Mantle chemical composition is more important for the alkaline olivine genesis of continental basalts. In this respect, geotectonic events and the formation depth of magma in the asthenosphere or lithospheric mantle are interdependent and important. In intracontinental basins, melts mainly originate from the convective asthenosphere (deep plumes) or the subcontinental lithospheric mantle (Ellam, 1992; McKenzie and O'Nions, 1995). Zindler and Hart (1986) interpret mantle sources in intercontinental basalts as the mixing of two or more end-member reservoirs of mantle DMM-depleted MORB, HIMU, and enriched mantle (i.e., EM1 and EM2). Wilson (1989) suggests asthenospheric mantle OIB and MORB in the petrogenesis of basalts in the intracontinental rift zones. According to McKenzie and O'Nions (1995), the intercontinental alkali basalts were formed from enriched lithospheric sources. They attribute this enrichment to the separation of small melts originating from the MORB source mantle. Yb is an element compatible with garnet and incompatible with spinel. Therefore, the enrichment of this element occurs only when garnet is the residual phase in the source area (Peters et al., 2008). Nevertheless, the average ratio of (Dy/Yb) in the basalts of the area is around 1.2. Usually, the high depletions of HREEs with (Dy/Yb) > 1.6 indicate the presence of garnet in the source area (Haase et al., 2004). However, this indicates that garnet does not play a role in the origin of the magmatic rocks in the study area (Lucassen et al., 2008).
In the diagram of N(Tb/Yb) versus N(La/Sm), all the samples of the study area have N $<$ 1.8(Tb/Yb) and show a spinel peridotite mantle source (Fig. 12 c). Values of N

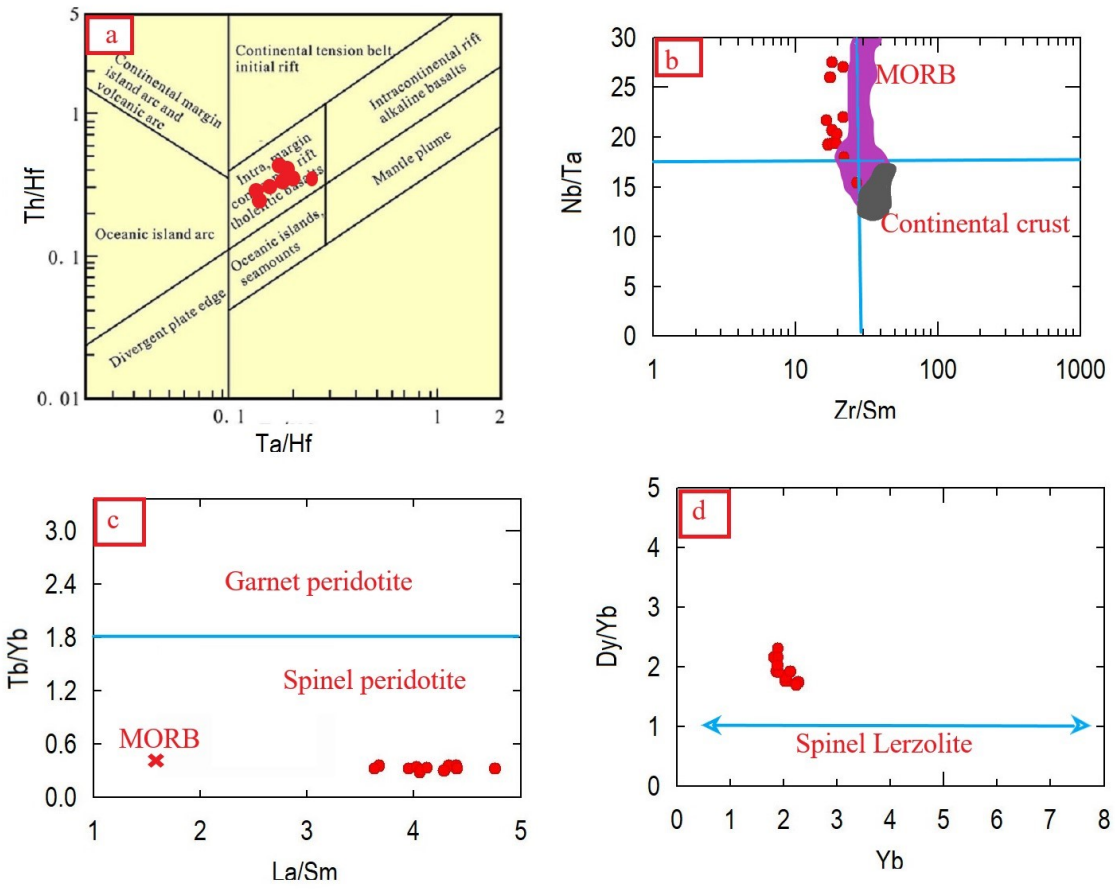

Figure 12. A- Position of samples on The Ta/Hfe vsTh/Hf discrimination diagram of the rocks (after Wang et al. (2002)). B- Position of samples on Nb/Ta versus Zr/Sm plot, from Foley et al. (2003). c- the position of samples in the diagram of Wang et al. (2002). d- Partial melting percentage of alkali olivine of Tarom basalts in the Dy/Yb versus Yb diagram, from Yan et al. (2018).

$<$ 1.8 (Tb/Yb) suggest a spinel-rich mantle (Wang et al., 2002). Fig. 12 (d) presents the Dy/Yb versus Yb diagram by Yan et al. (2018). The diagram shows the partial melting percentages of a lherzolitic spinel source. The data of the study area indicates the partial melting of approximately 15% from a lherzolitic spinel source.

The spinel-garnet gradation zone in the mantle is at a depth of approximately 65 km and a pressure range of $2-3.5$ GPs (McKenzie and Bickle, 1988). Therefore, the lherzolitic spinel facies are present at pressures less than 65 km and less than 20 kbar. Since Spinel lherzolite exists in oceanic areas up to a maximum depth of 75 km and in continental areas up to a maximum depth of 50 km (Brown and Most, 1981), the depth range of origin of basalts in the region should probably be less than 50 km. Experimental studies by Jaques and Green (1980) have shown that alkali olivine basalt is formed through the melting of a spinel peridotite at a pressure of 15 kbar (at a depth of approximately 50 km) and a partial melting rate of 15%. Likewise, Kushiro (1972) concluded that the melting of spinel peridotite without phlogopite (i.e., without water) occurs at a pressure of 15 kbar. According to Wilson (1989), the MORB source asthenospheric mantle shows the highest extensional activity in the petrogenesis of intracontinental rifts; this issue is observed in the Afar rift volcanic rocks in Ethiopia. In the study area, his rift is related to the presence of a hot spot under Azerbaijan that did not reach the evolution stage during the Eocene, like the Red Sea, and stopped before generating tholeiitic magma and oceanic crust. According to Lescuyer and Riou (1976), the transformation of the intracontinental rift in the Tarom and Azerbaijan regions at the end of the Eocene, due to the first movement of the opening of the Red Sea, remained uncontaminated and stopped before generating tholeiitic magma and oceanic crust. Regarding the alkaline nature of rocks in the region, the role of digesting carbonate rocks should also be considered. In other words, the rocks before the contamination might have lower alkalinity than the existing rocks. Therefore, we believe that due to magmas originating from the MORB source mantle, the basaltic magmas were contaminated by the lower crust.

6.3 Determining the tectonic setting of the Tarom Mountains in the Cenozoic

The Tarom mountain range is generally composed of Paleogene and Neogene rock units. This range is a large-scale anticline with small-scale folds intruded by numerous intrusive masses from the late Eocene onward. Between the mountains of Tarom and Talesh, there is a subsidence area that starts from the east of Manjil and extends parallel to the mountain range of Tarom to Firouzkoh. This subsidence area consists of Neogene sediments deposited in a shallow environment. The set of Paleogene rock units and folded

Neogene sediments are cut by important large-scale reverse faults on the edge of the Neogene sediments basin. The tectonic setting of the Tarom mountain range during different periods is categorized based on the rock units' characteristics and the Tarom range's structures.

In the last decade, several studies have been conducted on the tectonic setting of the igneous rocks in the Tarom region (Ashja Ardalan and Emami, 2005; Mafi et al., 2011; Castro et al., 2013; Nadri et al., 2013; Rahmani et al., 2018; Seyed Qaraini et al., 2019) however, the results are inconsistent to some extent. Comparing the location of the conducted studies and the results presented by different researchers indicates that the works conducted on the northern slopes of Tarom mountains are different from those on the southern slopes.

6.4 Studies conducted on the northern slopes of the Tarom mountains

Yazdi et al. (2005) investigated the northern slope of the Tarom mountains in the Badamestan region. The results showed that the range of changes of volcanic and plutonic rocks of Tarom starts from sub-alkaline and progresses to alkaline rocks rich in potassium and even onto shoshonites. The abundance of trace elements such as Ba, Rb, and Sr in the region's rocks can prove their alkaline and shoshonite properties. Due to features such as the alkaline and

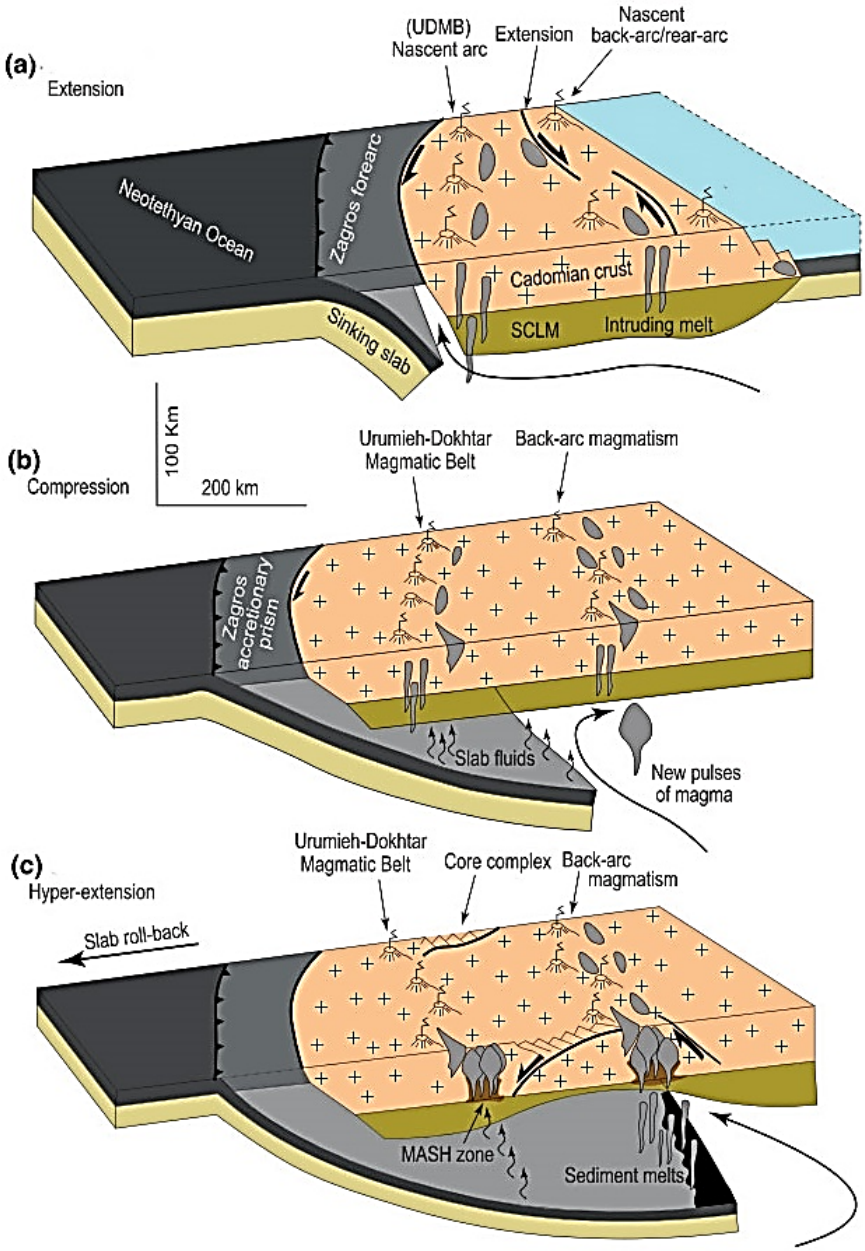

Figure 13. (a–c) Simplified cross-section of the Late Cretaceous-Paleogene convergent margin of Iran, showing different magmatic events in the North Iran back-arc magmatic belt. These panels emphasize the positions of the magmatic front and back arc; slab fluids triggering magmatic front magmatism versus sediment melts triggering back-arc magmatism, Subcontinental Lithospheric Mantle (SCLM), and Melting-Assimilation-Storage-Homogenization (MASH) processes beneath both magmatic front and back-arc (Shafaii Moghadam et al., 2020).

shoshonitic rocks of the region, their high alumina content, low titanium percentage, richness in LILE such as Rb, Ba, and Sr, the origin and depth of the magma of the rocks of the region, and the dependence of the rocks on each other, the region is comparable to back-arc volcanic and continental ridge basins. The results of Haghnazar and Shafeie (2014); Mafi et al. (2011) in Dehneh,Castro et al. (2013) on the northern slopes of the Tarom mountains, Yazdi et al. (2005) in ChahGhale-Badamestan, and Ashja Ardalan and Emami (2005) in the Kuhian area suggest that the eruptions occurred in their respective study areas incomplete rifts. In the late Eocene-Oligocene, due to the collisional movements in Central Iran and Alborz, these developments (rift magmatism) have remained incomplete (Nadri et al., 2013; Castro et al., 2013; Seyed Qaraini et al., 2019). In this respect, due to compressive movements, post-tectonic intrusive masses have penetrated them simultaneously and after tectonic movements. This zone is named Area A in Fig. 14.

6.5 Studies conducted on the southern slopes of the Tarom mountains

Kamali et al. (2011) in the south of Ghaflankouh, Ebrahimi et al. (2016) in the Aghkand area, Khademian et al. (2018) in the Amand area, Khalatbari Jafari et al. (2016), Esmaili et al. (2001) in Khalifelou area in the north of Abhar, Nadri et al. (2013) in the Zakir-Sorkh Dizaj range, and Sadri Esfanjani et al. (2014) the volcanic rocks in this areas have that have calc-alkaline characteristics with a meta-aluminous to shoshonitic composition. They also showed that the igneous assemblages of the southern and southwestern slopes of Tarom have erupted in a magmatic arc of the active continental margin affected by subduction zones. According to Seyed Qaraini et al. (2019), the information obtained from field studies, lithologies, geochemistry, and tectonic environment differentiation diagrams indicate that the intrusive masses of the Zajkan region are related to an enriched lithospheric mantle related to subduction and probably a post-collision basin. Khalatbari Jafari et al. (2016), in studying the petrography and geochemistry of the igneous rocks of the Aghdagh region in the northeast of Abhar (which are the eruptions of the Kurd Kand unit), reported that the volcanic eruptions of the Aghdagh area have occurred during five stages in an oceanic-continental basin. These eruptions have generated basic-intermediate and volcanic deposits with a basaltic composition, including andesite, trachyte-andesite, trachyte-trachydacite, dacite, and rhyolite. In the Aghdagh region, located on the southern side of the Tarom mountains, intermediate and acidic volcanic units are more extensive than basic units (Khalatbari Jafari et al., 2016). These outcrops have an NW-SE trend, which is folded into thrusts and anticlines. Based on the paleontological investigations, microfossils with middle-late Eocene age have been identified in the micrite limestones within the volcanic-sedimentary series. The results show that the volcanic activities in the Aghdagh region occurred during the middle-upper Eocene. Volcanic activities in this area started with the eruption of rhyolitic-dacite lavas. These activities were repeated intermittently and upward with intermediate basic lavas. In the Aghdagh region, evidence of hybrid fractures and magmatic mixing can also be found in rock units' Intermediate and acidic compositions.

Based on petrographic studies, these rocks show evidence of magmatic miscibility and mixing, including basic-intermediate fragments in the acidic matrix, plagioclase with sieve texture, honeycomb structure, oscillatory zoning, and dissolution margins. These lavas contain large amounts of K_2O and show calc-alkaline, high-potassium calc-alkaline, and shoshonite magmatic trends. The magmatic differentiation might have occurred in Three differ-

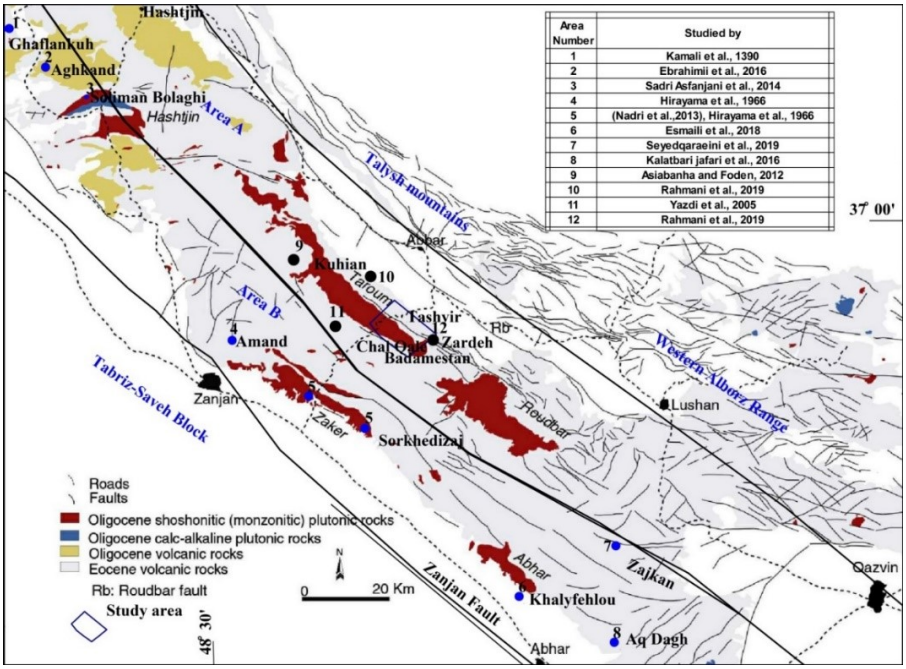

Figure 14. Location of petrological studies conducted in the Tarom Mountains; according to these studies, the Tarom area in the Eocene is divided into two parts: northern incomplete rift basin (Area A) and magmatic arc (Area B).

ent processes or stages from basic rocks toward acidic rocks. The intrusive masses of the Aghdagh region (Khalatbari Jafari et al., 2016; M. et al., 2016) are part of type-I active continental margins and belong to the hybrid type of magmatic arc of the active continental margin. Petrological studies on the intrusive masses (Castro et al., 2013; Seyed Qaraini et al., 2019; Nadri et al., 2013) belonging to the late Eocene-Oligocene, in the northern and southern slopes of the Tarom Mountains, have had almost similar results. According to these studies, these masses are related to the continental margin and the type of active continental arc. However, some researchers attributed hybrid characteristics to these masses. This zone is named Area B in Fig. 14. Therefore, the Tarom mountains can be divided into two parallel sub-zones: south and north. From the tectonic point of view, the southern sub-zone was the magmatic arc of the active continental margin in the Eocene period, and the northern sub-zone is located in the back-arc with stretching movements. The back-arc basin continued in it until the incomplete rift, and due to the compressive movements between Central Iran and the Turan Plate, the expansion of the rift did not continue much. The effects of these compressive movements are associated with the intrusion of granitoid masses of continental arcs or monzonites. A large amount of magma erupted due to the large volume of eruptions in the late Eocene. As magma cools down, ground subsidence has occurred in the Manjil-Gilvan-Daram area, and Tertiary sediments have been deposited in this area. Figure 15 shows the formation of rocks in the study area schematically.

7. Conclusion

1. In some thin sections, apatite and olivine minerals were observed in a dynamic-clitic form inside clinopyroxenes. This result suggests that they crystallized before the clinopyroxenes of these two minerals compared to clinopyroxenes. In addition, some olivines appear as poikilitic crystals surrounding euhedral apatites. This observation also reflects the apatite crystallized before olivine and pyroxene.
2. In the diagram of SiO_2 against Zr/Ti by Winchester and Floyd (1977) and Yoder and Tilley (1962), all samples are located in the range of alkaline basalts. In weight norm estimations, olivine was calculated along with nepheline. The amount of nepheline is less than 5%, and the value of Mg# in the samples varies between 55.5 and 46.5. These observations suggest the evolution of olivine in the alkaline basalts of the region. In the chart of SiO_2 against Mg#, a decrease in the amount of SiO_2 can be seen along with a decrease in Mg# and an increase in crystalline differentiation. This result suggests that following the assimilation of carbonate rocks by magma, Si and Mg were consumed to make clinopyroxene in the magma.
3. The results showed some fluctuations and consistency of the elemental trend of the basalts of the region with the underlying continental crust, suggesting the contamination of these rocks with the continental crust. Also, the K_2O/Na_2O and Ba/Rb values in the olivine basalts of the study area indicate a rift system origin for these rocks.
4. The magmatic series of the volcanic and plutonic rocks of the study area are calc-alkaline with high potassium and they are shoshonitic in nature. Also, they are enriched with trace elements such as Th, Sr, Ba, Rb, and K.
5. The Tarom mountains can be divided into two subzones: southern and northern. In the Eocene period, the southern sub-zone was the tectonic setting of the magmatic arc of the active continental margin. In addition, the northern sub-zone was the back-arc. The extension of the back-arc basin has continued to untile an incomplete rift. However, due to the compressive movements between the Central Iran and Turan plates, the extension of the rift has not continued much. The

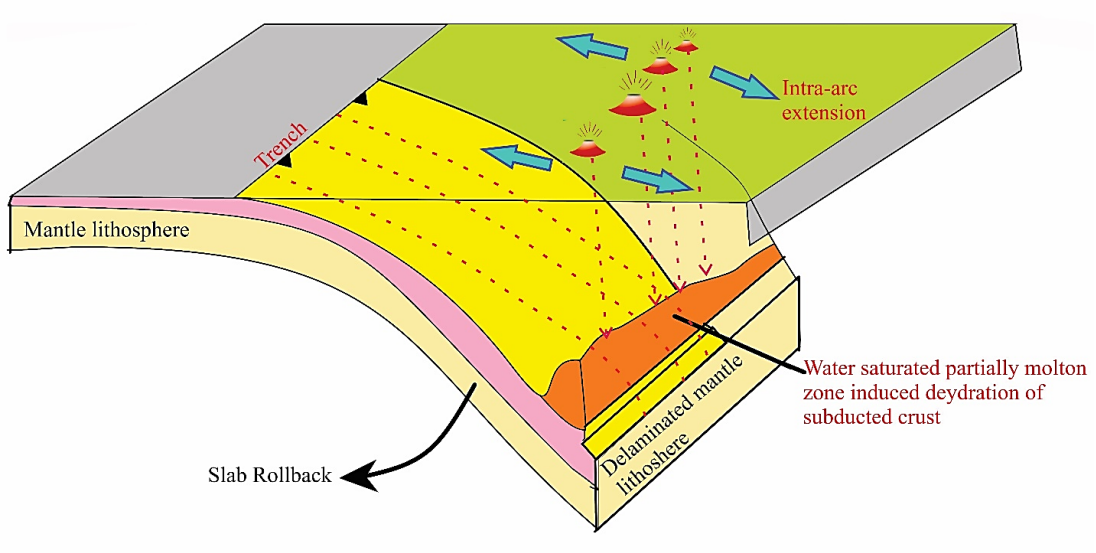

Figure 15. Schematic figure of the formation of rocks in the studied area.

intrusion of granitoid masses of continental arcs or Oligo to Miocene monzonites has accompanied the effects of these compressive movements. Due to the large eruptions in the late Eocene, a large amount of magma erupted. As a result, the gradual subsidence of the lands in the Manjil-Gilvan-Dram area continued, and Tertiary sediments were deposited in this subsided area. The exact interpretation of the sequence of these processes will be possible after determining the exact age of igneous Eocene rocks, late Eocene-Oligocene intrusive masses, and Neogene sediments.

6. Regarding the alkaline nature of the rocks in the region, it is necessary to incorporate the role of the assimilation of carbonate rocks. In other words, before the contamination, the rocks might have had lower alkalinity than the current rocks. This rift is related to the presence of a thermal hot spot in the territory of Azerbaijan, which did not reach the stage of evolution during the Eocene, unlike the Red Sea, and stopped before generating the tholeiitic magma and oceanic crust.

Authors contributions
Authors have contributed equally in preparing and writing the manuscript.

Availability of data and materials
The data that support the findings of this study are available from the corresponding author, upon reasonable request.

Conflict of interests
The authors declare that they have no known competing financial interests or personal relationships that could have appeared to influence the work reported in this paper.

References

Abdolahadi A., Sheikhzakariaee S. J., Yazdi A., Mousavi S. Z. (2025) Plio-Quaternary Adakite Genesis and Post-collisional Processes: Whole Rock Constraints and Sr, Nd Isotopic Compositions in Alborz Magmatic Belt, Ardabil, Iran. *Journal of Mining and Environment* 16 (2): 737–765. DOI: https://doi.org/10.22044/jme.2024.14781.2801.

Alavi M. (1996) Tectonostratigraphic synthesis and structural style of the Alborz Mountain system in northern Iran. *Geodynamics* 21:1–33.

Allen M., Ghassemi M. R., Shahrabi M., Qorashi M. (2003) Accommodation of late Cenozoic oblique shortening in the Alborz Range, northern Iran. *Journal of Structural Geology* 25 (5): 659–672. DOI: https://doi.org/10.1016/S0191-8141(02)00064-0.

Ashja Ardalan A., Emami M. H. (2005) Petrological study of Tarom Olia plutonism (kohian area). *Journal of Sciences (Islamic Azad University)* 15:250–270. in Persian

Ashrafi N., Dabiri R., Jahangiri A. (2024) Some chemical variations in biotite, phlogopite, and muscovite, considering their tectonic setting. *Geopersia* 14 (2): 307–332. DOI: https://doi.org/10.22059/geope.2024.373882.648749.

Asiabanha A., Foden J. (2012) Post-collisional transition from an extensional volcano-sedimentary basin to a continental arc in the Alborz Ranges, N-Iran. *Lithos* 148:98–111. DOI: https://doi.org/10.1016/j.lithos.2012.05.014.

Barnes C. G., Prestvik T., Sundvoll B., Surratt D. (2005) Pervasive assimilation of carbonate and silicate rocks in the Hortavær igneous complex, north-central Norway. *Lithos* 80:179–199.

Berberian M., King G. C. P. (1981) Towards a paleogeography and tectonic evolution of Iran. *Canadian Journal of Earth Sciences* 18 (2): 210–265.

Borisova A. Y., Belyatsky B. V., Portnyagin M. V., Sushchevskaya N. M. (2001) Petrogenesis of olivine-phyric basalts from the Aphanasey Nikitin Rise: evidence for contamination by cratonic lower continental crust. *Journal of Petrology* 42 (2): 277–319. DOI: https://doi.org/10.1016/j.lithos.2003.11.002.

Brown G. C., Most A. E. (1981) The Inaccessible Earth. *Allen and Unwin, London,* 235p.

Brunet M. F., Korotaev M. V., Ershov A. V., Nikishin A. M. (2003) The South Caspian Basin: a review of its evolution from subsidence modeling. *Sedimentary Geology* 156:119–148. DOI: https://doi.org/10.1016/S0037-0738(02)00285-3.

Carlson R. W. (1991) Physical and chemical evidence on the cause and source characteristics of flood basalt volcanism. *Australian Journal of Earth Sciences* 38:525–544.

Castro A., Aghazadeh M., Badrzadeh Z., Chichorro M. (2013) Late Eocene–Oligocene post-collisional monzonitic intrusions from the Alborz magmatic belt, NW Iran. An example of monzonite magma generation from a metasomatized mantle source. *Lithos* 180:109–127. DOI: https://doi.org/10.1016/j.lithos.2013.08.003.

Condie K. C. (2005) High field strength element ratios in Archean basalts: a window to evolving sources of mantle plumes?. *Lithos* 79:491–504. DOI: https://doi.org/10.1016/j.lithos.2004.09.014.

Cox K. G., Bell J. D., Pankhurst R. J. (1979) The interpretation of igneous rocks. *George Allen and Unwin, London,* 450p.

Cox K. G., Hawkesworth C. J. (1985) Geochemical stratigraphy of Deccan Traps, at Mahabalshwar, western Ghats, India, with implication for open system magmatic processes. *Journal of Petrology* 26:355–377.

Dabiri R., Akbari-Mogaddam M., Ghaffari M. (2018) Geochemical evolution and petrogenesis of the Eocene Kashmar granitoid rocks, NE Iran: Implications for fractional crystallization and crustal contamination processes. *Iranian Journal of Earth Sciences* 10 (1): 68–77.

DeCelles P. G., Ducea M. N., Kapp P., Zandt G. (2009) Cyclicity in Cordilleran orogenic systems. *Nature Geoscience* 2 (4): 251–257. DOI: https://doi.org/10.1038/ngeo469.

Dedual E. (1967) Zur Geologie Dest Mittleren Und Unteren Karaj-Tales, Zentral Elburz (Iran). *Unpublished Ph.D. Thesis, University of Zurich, Zurich,* 125 pp. (in German)

Ducea M. N., Paterson S. R., DeCelles P. G. (2015) High-volume magmatic events in subduction systems. *Elements* 11 (2): 99–104. DOI: https://doi.org/10.2113/gselements.11.2.99.

Ebrahimi M., Kohestani H., Mokhtari M. A. A., Faizi M. (2016) Petrology and geochemistry of acidic volcanic rocks and perlites of Aqkand, north of Zanjan. *Earth Sciences Quarterly* 101:99–110. DOI: https://doi.org/10.22071/gsj.2016.41039.

Ellam R. M. (1992) Lithospheric thickness as a control on basalt geochemistry. *Geology* 20:153–156.

Elmi R., Arian M. A., Ashja Ardalan A., Yazdi A. (2025) Petrology of volcanism in the Alasht-Haraz road of the Alborz mountain range, south of Amol (north of Iran). *Iranian Journal of Earth Sciences* 17 (3) DOI: https://doi.org/10.57647/j.ijes.2025.16800.

Emami M. H. (2000) Magmatism in Iran. *Geological Survey of Iran, Tehran,* in Persian

Esmaili M., Lotfi M., Nazafti N. (2001) Mineralogy and genesis of Khalifalu copper deposit based on geochemical data of the host rock and S and O isotopic characteristics. *Earth Sciences Quarterly* 110:33–46. DOI: https://doi.org/10.22071/gsj.2019.84248.

Farahat E. S., Ghani M. S. A., Aboazom A. S., Asran A. M. H. (2006) Mineral chemistry of Al Haruj low-volcanicity rift basalts, Libya: implications for petrogenetic and geotectonic evolution. *Journal of African Earth Sciences* 45 (2): 198–212. DOI: https://doi.org/10.1016/j.jafrearsci.2006.02.007.

Ferrari L., Lopez-Martinez M., Orozco-Esquivel T., Bryan S. E., Duque-Trujillo J., Lonsdale P., Solari L. (2013) Late Oligocene to Middle Miocene rifting and synextensional magmatism in the southwestern Sierra Madre Occidental, Mexico. The beginning of the Gulf of California rift. *Geosphere* 9 (5): 1161–1200. DOI: https://doi.org/10.1130/GES00925.1.

Fitton J. G., Saunders A. D., Norry M. J., Hardarson B. S., Taylor R. N. (1997) Thermal and chemical structure of the Iceland Plume. *Earth and Planetary Science Letters* 153:197–208.

Foley S., Buhre S., Jacob D. E. (2003) Evolution of the Archaean crust by delamination and shallow subduction. *Nature* 417:837–840. DOI: https://doi.org/10.1038/421230b.

Ghasempour M. R., Ghazi J. M., Biabangard H., Dabiri R. (2015) Petrogenic significance of the Plio-Quaternary Nehbandan mafic lavas, Eastern Iran. *Iranian Journal of Earth Sciences* 6 (2): 133–141.

Ghorbani M. (2013) The Economic Geology of Iran. *Springer,* 581 pp.

Haase K. M., Goldschmidt B., Garbe-Schönberg C. D. (2004) Petrogenesis of tertiary continental intraplate lavas from the Westerwald region, Germany. *Journal of Petrology* 45 (5): 883–905. DOI: https://doi.org/10.1093/petrology/egg115.

Haghnazar S., Shafeie Z. (2014) The role of MORB-mantle source and continental crust in the genesis of Tertiary volcanic rocks of Nash area in the east of Roudbar, North of Iran. *Petrology* 4 (15): 39–54. in Persian

Hakimi Asiabar S., Bagheriyan S. (2018) Exhumation of the Deylaman fault trend and its effects on the deformation style of the western Alborz belt in Iran. *International Journal of Earth Sciences* 107 (2): 539–551. DOI: https://doi.org/10.1007/s00531-017-1507-4.

Hakimi Asiabar S., Pourkermani M., Shahriari S., Ghorbani M., Ghasemi M. R. (2011) Geological zones of western Alborz Mountains. *Journal of Sciences Islamic Azad University* 21 (81): 113–124.

Hirayama K., Samimi M., Zahedi M., HushmandZadeh A. (1966) Geology of the Tarom District, Western Part (Zanjan area northwest Iran). *Geological Survey of Iran Report* 8 31 p.

Hoffer G., Eissen J.-P., Beate B., Bourdon E., Fornari M., Cotten J. (2008) Geochemical and petrological constraints on rear-arc magma genesis processes in Ecuador: The Puyo cones and Mera lavas volcanic formations *J. Volcanol. Geotherm. Res.* 176:107–118. DOI: https://doi.org/10.1016/j.jvolgeores.2008.05.023.

Hoffman A. M. (1997) Mantle geochemistry: The messages from oceanic volcanism. *Nature* 385:219–229.

Hofmann A. W., Jochum K. P., Seufert M., White W. M. (1986) Nb and Pb in oceanic basalts: new constraints on mantle evolution. *Earth and Planetary Science Letters* 79:33–45.

Holm P. E. (1985) The Geochemical Fingerprints of different tectonomagmatic environments using hygromagmatophile element abundances of tholeiitic basalts and basaltic andesites. *Chemical Geology* 51:303–323.

Jamalomidi R., Hakimi Asiabar S., Haghnazar S., Vosoghi Abedini M. (2022) Tectonic environment and petrogenesis of igneous rocks of Tashvir area, Tarom mountains, northwest of Iran. *Geosciences* 32 (124): 105–120. DOI: https://doi.org/10.22071/gsj.2022.305126.1936.

Jaques A. L., Green D. H. (1980) Anhydrous melting of peridotite at 0-15 Kb pressure and the genesis of tholeiitic basalts. *Contrib Mineral Petrology* 73:287–310.

Kamali A., Moayed M., Jahangiri A., Amel N., Pirouj H., Ameri A. (2011) Study of petrography and geochemistry of volcanic rocks of Kaifalan mountain (northwest of Iran). *Journal of Petrology* 2:97–115.

Kamenov B., Yanev Y., Nedialkov R., Moritz R., Peytcheva I., Von Quadt A., Stoykov S., Zartova A. (2004) An across-arc petrological transect through the Central Srednogorie Late-Cretaceous magmatic centers in Bulgaria. *Bulg Geol Soc Annual Scientific Conference "Geology 2004", Proceedings,* 35–37.

Kampunzu A. B., Mohr P. (1991) Magmatic evolution and petrogenesis in the east African rift system. In: Kampunzu, A. B. and Lubala, R. T. (Eds.): Magmatism in extensional structural settings: The phanerozoic African plate. Springer

Keskin M., Pearce J. A., Mitchell J. G. (1998) Volcano stratigraphy and geochemistry of collision-related volcanism on the Erzurum-Kars Plateau, North Eastern Turkey. *Journal of Volcanology and Geothermal Research* 85:355–404.

Khademian F., Monsef A., Rahgoshai M. (2018) Petrology and geochemistry of the Eocene volcanic sequence in the northeast of Zanjan: with a perspective on the magmatism of the active continental boundary in the Alborz-Azerbaijan zone. *Journal of Petrology* 9 (1)

Khalatbari Jafari M., Akbari M., Ghalamghash J. (2016) Geology, Petrology and Tectonomagmatic Evolution of the Eocene Volcanic Rocks in Aq Dag Area, NE Abhar. *Kharazmi Journal of Earth Sciences* 2 (1): 33–60.

Kurt H., Asan K., Ruffet G. (2008) The relationship between collision-related calc-alkaline, and within plate alkaline volcanism in the Karacadag Area (Konya- Turkiye, Central Anatolia). *Chemie der Erde* 68:155–176.

Kushiro I. (1972) Effect of water on the composition of magmas formed at high pressures. *Journal of Petrology* 13:311–334.

Lescuyer J. L., Riou R. (1976) Geologie de la region de mineh (Azerbaijan) Contribution a l'etude du volcanisme tertiaire de l'Iran. *These de 3eme Cycle Grenoble,* 233 p.

Li B., Bagas L., Gallardo L. A., Said N., Diwu C., McCuaig T. C. (2013) Back-arc and post-collisional volcanism in the Palaeoproterozoic Granites-Tanami Orogen, Australia. *Precambrian Research* 224:570–587. DOI: https://doi.org/10.1016/j.precamres.2012.11.002.

Lucassen F., Franz G., Romer R. L., Pudlo D., Dulski P. (2008) Nd, Pb and Sr isotope composition of late Mesozoic to Quaternary intraplate magmatism in NE- Africa (Sudan, Egypt): high - μ signatures from the mantle lithosphere. *Contributions to Mineralogy and Petrology* 156:756–784.

M. Khalatbari Jafari, M. Akbari, J. Ghalamghash (2016) Geology, Petrology and Tectonomagmatic Evolution of the Eocene Volcanic Rocks in Aq Dag Area, NE Abhar. *Kharazmi Journal of Earth Sciences* 2:33–60.

Mafi H., Ghorbani M., Rezaei Kokhaei M. (2011) Petrology of Volcanic Rocks of Upper Tarem, Dehne Field. *30th Earth Sciences Meeting, Tehran*

Mason B., Moore C. (1982) Principles of Geochemistry. *Kharazmi Journal of Earth Sciences* Wiley, New York:345.

McDonough W. F., Frey F. A. (1989) Rare earth elements in upper mantle rocks. *Geochemistry and mineralogy of rare earth elements,* 99–146.

McKenzie D., Bickle M. J. (1988) The volume and composition of melt generated by extension of the lithosphere. *Journal of Petrology* 29:625–679.

McKenzie D., O'Nions R. K. (1995) The source regions of ocean island basalts. *Journal of Petrology* 36:133–159.

Middlemost E. A. K. (1975) The basalt clan. *Earth-Science Reviews* 11:337–564.

Mollo S., Gaeta M., Freda C., Di Rocco T., Misiti V., Scarlato P. (2010) Carbonate assimilation in magmas: A reappraisal based on experimental petrology. *Lithos* 117:503–514.

Nabavi M. H. (1976) An introduction to the geology of Iran. *Geological Survey of Iran,* 109 p. (In Persian)

Nadri M., Rashidenjademaran N., Aghazadeh M. (2013) Geochemistry, origin and geodynamic environment of Zakir-Sarkheh Dizj intrusive mass, southern slope of Tarem sub-zone, east of Zanjan. *Khwarazmi University Science Journal* 31 (4): 951–972.

Nazari Sarem M., Vosoghi Abedini M., Dabiri R., Ansari M. R. (2021) Geochemistry and petrogenesis of basic Paleogene volcanic rocks in Alamut region, Alborz mountain, north of Iran. *Earth Sciences Research Journal* 25 (2): 237–245.

Ousta S. H., Ashja-Ardalan A., Yazdi A., Dabiri R., Arian M. A. (2024) Petrogenesis and tectonic implications of Miocene dikes in the south-east of Bam (SE Iran): Constraints on the development of active continental margin. *Geopersia* 14 (1): 89–111.
DOI: https://doi.org/10.22059/geope.2023.364334.648729.

Pearce J. A. (2008) Geochemical Fingerprinting of Oceanic Basalts with Applications to Ophiolite Classification and the Search for Archean Oceanic Crust *Lithos* 100:14–48.
DOI: https://doi.org/10.1016/j.lithos.2007.06.016.

——— (1983) Role of sub-continental lithosphere in magma genesis at active continental margins. *In Hawkesworth, C.J. and Norry, M.J. (eds) Continental basalts and mantle xenoliths, Shiva, Nantwich,* 230–249.

——— (1982) Trace element characteristics of lavas from destructive plate boundaries. *In Thorpe R.S. (ed) Andesites, Wiley, Chichester,* 525–548.

Peccerillo A. (1999) Multiple mantle metasomatism in central-southern Italy: geochemical effects, timing and geodynamic implications. *Geology* 27:315–318.

Peters T. J., Menzies M., Thirlwal M., Kyle P. K. (2008) Zuni- Bandera volcanism, Rio Grande, USA, Melt formation in garnet-and spinel-facies mantle straddling the asthenosphere –lithosphere boundary. *Lithos* 102:295–315.

Rahmani S., Hassan Zamaniyan H., Zarei Sahamiyeh R. (2018) Geochemical characteristics of igneous rocks related to Lubin-Zardeh epithermal gold deposit, Northwest Iran. *Journal of Geochemical Exploration* 114:289–302.

Reichow M. K., Saunders A. D., White R. V., Al'Mukhamedov A. I., Medvedev A. Ya. (2005) Geochemistry and petrogenesis of basalts from the West Siberian Basin: an extension of the Permo–Triassic Siberian Traps, Russia. *Lithos* 79 (3-4): 425–452.
DOI: https://doi.org/10.1016/j.lithos.2004.09.011.

Ritz J. F., Nazari H., Salamati R., Shafeii A., Solaymani S., Vernant P. (2006) Active transtension inside Central Alborz: a new insight into the Northern Iran–Southern Caspian geodynamics. *Geology* 34 (5): 477–480.

Rudnick R. L., Fountain D. M. (1995) Nature and composition of the continental crust: A lower crustal perspective. *Reviews of Geophysics* 33 (3): 267–300.

Ryan J., Morris J., Bebout G., Leeman B. (1996) Describing Chemical Fluxes in Subduction Zones: Insights from "Depth-Profiling" Studies of Arc and Forearc Rocks. *In: Bebout, G. E. and Scholl, D. W. and Kirby, S. H. and Platt, J. P. (Eds), Subduction Top to Bottom, American Geophysical Union, Washington DC,* 263–268.

Sadri Esfanjani S., Amel N., Mokhtari M. A. A. (2014) Petrology and geochemistry of acid volcanic rocks in the north of Sulaimanbalaghi (southwest of Hashtjin, north of Zanjan), with a perspective on perlite. *Journal of Petrology* 21:139–156.

Salehpour S., Arian M. A., Rad A. J., Zarei Sahamieh R., Yazdi A. (2025) Geochemistry and technomagmatic environment of Eocene volcanic rocks in Yuzbashi Chay region, west of Qazvin (Iran). *Iranian Journal of Earth Sciences* 17 (1): 1–13.
DOI: https://doi.org/10.57647/j.ijes.2025.1701.04.

Saunders A. D., Norry M. J., Tarney J. (1988) Origin of MORB and chemically-depleted mantle reservoirs: Trace element constraints. *Journal of Petrology* 1:415–445.

Seebeck H., Nicol A., Giba M., Pettinga J., Walsh J. (2014) Geometry of the subducting Pacific plate since 20 Ma, Hikurangi margin, New Zealand. *Journal of the Geological Society* 171 (1): 131–143.

Sepidbar F., Shafaii Moghadam H., Zhang L., Li J. W., Ma J., Stern R. J., Lin C. (2019) Across-arc geochemical variations in the Paleogene magmatic belt of Iran. *Lithos* 344-345:280–296.

Seyed Qaraini A., Mokhtari M. A., Kohestani H. (2019) Petrology, geochemistry and tectonomagmatic setting of Zajkan granitoid, Tarom-Hashtjin sub-zone, West of Qazvin. *Petrology of Isfahan University* 10:79–100.

Shafaii Moghadam H., Li Q. L., Li X. H., Stern R. J., Levresse G., Santos J. F. (2020) Neotethyan Subduction Ignited the Iran Arc and Backarc Differently. *Journal of Geophysical Research: Solid Earth* 125 (7)

Shafeie Z., Arian M. A., Haghnazar S., Vossoughi Abedini M. (2016) Geochemistry and Petrogenesis of Tertiary Volcanic Rocks of the Eastern Roodbar, Alborz Mountain, North of Iran. *Open Journal of Geology* 6:1296–1311.

Shuqing S., Yunliang W., Chengjiang Z. (2003) Discrimination of the tectonic setting of basalts by Th, Nb and Zr. *Journal of Geology Research* 49:40–47.

Su B. X., Qin K. Z., Sun H., Tang D. M., Sakyi P. A., Chu Z. Y., Liu P. P., Xiao Q. H. (2012) Subduction-induced mantle heterogeneity beneath Eastern Tianshan and Beishan: insights from Nd–Sr–Hf–O isotopic mapping of Late Paleozoic mafic–ultramafic complexes. *Lithos* 134–135:41–51.

Sun J., Li N., Dong C. H., Yanhong R. (2022) Geochemical Features of Volcanic Rocks from the Shaerbuti Mountain Complex, West Junggar, Xinjiang, China: Implications for Recycling of Materials. *Journal of Minerals* 13 (75)

Sun S. S., McDonough W. F. (1989) Chemical and isotopic systematics of oceanic basalts: implication for mantle composition and processes. *Geological Society, London, Special Publications* 42:313–345.
DOI: https://doi.org/10.1144/GSL.SP.1989.042.01.19.

Tatsumi Y., Hamilton D. L., Nesbitt R. W. (1986) Chemical characteristics of fluid phase released from a subducted lithosphere and origin of arc magmas: evidence from high-pressure experiments and natural rocks. *Journal of Volcanology and Geothermal Research* 29:293–309.

Taylor S. R., McLennan S. M. (1985) The continental crust: its composition and evolution. *Blackwell, Oxford, England*

Thompson R. N., Morrison M. A., Hendry G. L., Parry S. J. (1984) An assessment of the relative roles of crust and mantle in magma genesis: an elemental approach. *Philosophical Transactions of the Royal Society A* 310:549–590.

Turner S., Hawkesworth C. J. (1995) The nature of the sub-continental mantle: constraints from the major element composition of continental flood basalts. *Chemical Geology* 120:295–314.

Verdel C. (2009) Cenozoic geology of Iran: an integrated study of extensional tectonics and related volcanism. *PhD thesis, California Institute of Technology,* 287 p.

Verma S. P. (2009) Continental rift setting for the central part of the Mexican volcanic belt: A statistical approach. *The Open Geology Journal* 3:8–29.

Vincent S. J., Allen M. B., Ismail-Zadeh A. D., Flecker R., Foland K. A., Simmons M. D. (2005) Insights from the Talysh of Azerbaijan into the Paleogene evolution of the South Caspian region. *Geological Society of America Bulletin* 117 (12): 1513–1533.

Wang J. H., Wang H., Chen H. S., Jiang S., Zhao S. E. (2013) Responses of two lithosomes of Lower Cretaceous coarse clastic rocks to tectonism in Kuqa foreland sub-basin, Northern Tarim Basin, Northwest China. *Sedimentary Geology* 289:182–193.

Wang K., Plank T., Walker J. D., Smith E. I. (2002) A Mantle Melting Profile across the Basin & Range, SW USA. *Journal of Geophysical Research* 107 (ECV 5): 1–21.

Wang Q., Deng J., Liu X., Zhang Q., Sun S., Jiang C., Zhou F. (2010) Discovery of the REE minerals and its geological significance in the Quyang bauxite deposit, West Guangxi, China. *Journal of Asian Earth Sciences* 39 (6): 701–712. DOI: https://doi.org/10.1016/j.jseaes.2010.05.005.

Weaver B. L. (1991) The origin of ocean island basalt end-member compositions: Trace element and isotopic constraints. *Earth and Planetary Science Letters* 104:381–397.

Whitney D. L., Evans B. W. (2010) Abbreviations for names of rock-forming minerals. *American mineralogist* 95 (1): 185–187.

Willson M., Downes H. (2006) Tertiary- Quaternary intra-plate magmatism in Europe and its relationship to mantle dynamics. *Geological Society* 32:147–166.

Wilson M. (1989) Igneous Petrogenesis: A Global Tectonic Approach. *Unwin Hyman, London,* 466p.

Winchester J. A., Floyd P. A. (1977) Geochemical Discrimination of Different Magma Series and Their Differentiation Product Using Immobile Elements. *Chemical Geology* 20:325–343.

Woodhead J. D., Hergt J. M., Davidson J. P., Eggins S. M. (2001) Hafnium isotope evidence for "conservative" element mobility during subduction zone processes: Earth and Planetary *Science Letters* 192:331–346. DOI: https://doi.org/10.1016/S0012-821X(01)00453-8.

Yan Q., Shi X., Metcalfe I., Liu S., Xu T., Kornkanitnan N., Sirichaiseth T., Yuan L., Zhang Y., Zhang H. (2018) Hainan mantle plume produced late Cenozoic basaltic rocks in Thailand, Southeast Asia. *Scientific Reports* 8 (2640) DOI: https://doi.org/10.1038/s41598-018-20712-7.

Yazdi A., Ashja-Ardalan A., Emami M. H., Dabiri R., Foudazi M. (2019) Magmatic interactions as recorded in plagioclase phenocrysts of quaternary volcanics in SE Bam (SE Iran). *Iranian Journal of Earth Sciences* 11 (3): 215–224. DOI: https://doi.org/10.30495/ijes.2019.667379.

Yazdi A., Emami M. H., Vathouqi Abedini M. (2005) Petrological study of Eocene volcanic rocks of Chal Qala Badamestan area (Upper Tarem, Zanjan province). *9th conference of Geological Society of Iran*

Yoder H. S., Tilley C. E. (1962) Origin of basalt magmas: an experimental study of natural and synthetic rock systems. *Journal of Petrology* 3:342–532.

Zanchi F., Berra M., Mattei M. R., Ghassemi M. R., Sabouri J. (2006) Inversion tectonics in central Alborz, Iran. *Journal of Structural Geology* 28 (11): 2023–2037. DOI: https://doi.org/10.1016/j.jsg.2006.06.020.

Zhang J. Y., Ma C. Q., Xiong F. H., Liu B. (2022) Petrogenesis and tectonic significance of the Late Permian–Middle Triassic calc-alkaline granites in the Balong region, eastern Kunlun orogen, China. *Geological Magazine* 149 (5): 892–908. DOI: https://doi.org/10.1017/S0016756811001142.

Zindler A., Hart S. R. (1986) Chemical geodynamics. *Earth and Planetary Science Letters* 14:493–571.